ISSN 1075-7015, Geology of Ore Deposits, 2006, Vol. 48, No. 3, pp. 215–236. © Pleiades Publishing, Inc., 2006.
Original Russian Text © S.V. Voroshin, E.E. Tyukova, N.A. Gibsher, 2006, published in Geologiya Rudnykh Mestorozhdenii, 2006, Vol. 48, No. 3, pp. 249–272.

Metamorphism of Sulfides and Gangue Quartz at the Degdekan and Gol'tsovsky Gold Deposits, Magadan Oblast

S. V. Voroshin[a], E. E. Tyukova[a], and N. A. Gibsher[b]

[a]*Northeast Complex Research Institute, Far East Division, Russian Academy of Sciences, ul. Portovaya 16, Magadan, 685000 Russia*

[b]*Institute of Mineralogy and Petrography, Siberian Division, Russian Academy of Sciences, pr. Akademika Koptyuga 3, Novosibirsk, 630090 Russia*

Received April 13, 2005

Abstract—The Degdekan and Gol'tsovsky gold–quartz deposits are located in the southeastern Yana–Kolyma gold belt. The orebodies occur as quartz veins hosted in metaterrigenous rocks and cut by postmineral basic–intermediate dikes. It was established that metamorphism of sulfides and gangue quartz was restricted to a few centimeters off the dike contact. According to sulfide geothermometers, the metamorphic temperatures close to the contact of dikes attained 700°C at the Degdekan deposit and were no higher than 491°C at the Gol'tsovsky deposit. The formation of the forbidden assemblage of quartz and loellingite and its fine-grained texture indicate that the thermal effect on the Degdekan ore was short-term. The prolonged heating of the ore at the Gol'tsovsky deposit gave rise to the aggradation recrystallization of quartz and the formation of equilibrium sulfide aggregates that show only insignificant differences in composition from the primary phases. The average homogenization temperature of primary and pseudosecondary fluid inclusions is 206 ± 40°C in the unmetamorphosed veins and 257 ± 33°C in the metamorphosed veins. The salinity of fluids in the primary and pseudosecondary inclusions in quartz veins of both types varies from 0.5 to 14.0 wt % NaCl equiv. The melting temperature of liquid CO_2 in the carbon dioxide inclusions, ranging from –57.0 to –60.8°C, suggests an admixture of CH_4 and/or N_2. The unmetamorphosed quartz veins were formed at a fluid pressure varying from 0.7 to 1.3 kbar, while quartz veins at the contact with dikes crystallized at a pressure of 0.8–1.5 kbar. The results of gas chromatography showed the presence of CO_2 and H_2O, as well as N_2 and CH_4. The average bulk of volatiles contained in the fluid inclusions in quartz from the metamorphosed veins is 1.5–2 times lower than in the unmetamorphosed veins; this proportion is consistent with the occurrence of decrepitated gas inclusions in the heated quartz.

DOI: 10.1134/S1075701506030044

INTRODUCTION

Since the discovery of the Yana–Kolyma gold belt in the 1930s, relationships between intrusive and hydrothermal rocks have been used to establish the sequence of geological events and the genesis of gold–quartz deposits. Special attention has been paid to ore metamorphism caused by the emplacement of younger granitoid bodies. Bilibin (1940) suggested an older age of the gold-bearing quartz veins relative to granitoids on the basis of field observations and microscopic examination of thin sections. In developing this concept, Skornyakov (1949) characterized the contact metamorphic alteration of mineral composition of the veins at the Vostochny, Zolotoi, Igumenov, Klin Tenisty, Rodionov, and other deposits. Comparison of the data with those for other gold-bearing occurrences in this region allowed him to reveal the general features of contact-metamorphosed veins. In elaborating these features, Firsov (1956, 1958) characterized the progressive stages of transformation of gangue quartz and native gold at the Rodionov and Igumenov deposits. However, the evidence for contact metamorphism of ore has subsequently been questioned (Anikeev et al., 1976; Shilo et al., 1988; Andreev et al., 1984).

This work was aimed at studying the transformation of quartz veins and sulfide assemblages at contacts with dikes at the Degdekan and Gol'tsovsky deposits using paragenetic analysis and thermobarogeochemical methods. The metamorphism of sulfides at the Degdekan deposit was partly characterized previously (Voroshin, 1988).

GEOLOGY OF THE DEPOSITS

Both deposits are situated in the southeastern Yana–Kolyma gold belt, which comprises vast areas of gold placers and numerous primary deposits and occurrences of gold–quartz, gold–antimony, and gold–tungsten mineralization (Fig. 1). The gold belt was formed in the Late Jurassic–Early Cretaceous as a result of collision of the Kolyma–Omolon Superterrane and the North Asian Craton. The belt embraces the passive margin of the North Asian Craton (the Verkhoyansky Fold–Thrust Belt), the Kular–Nera and Viliga pericra-

Corresponding author S.V. Voroshin. E-mail: sv@magis.ru

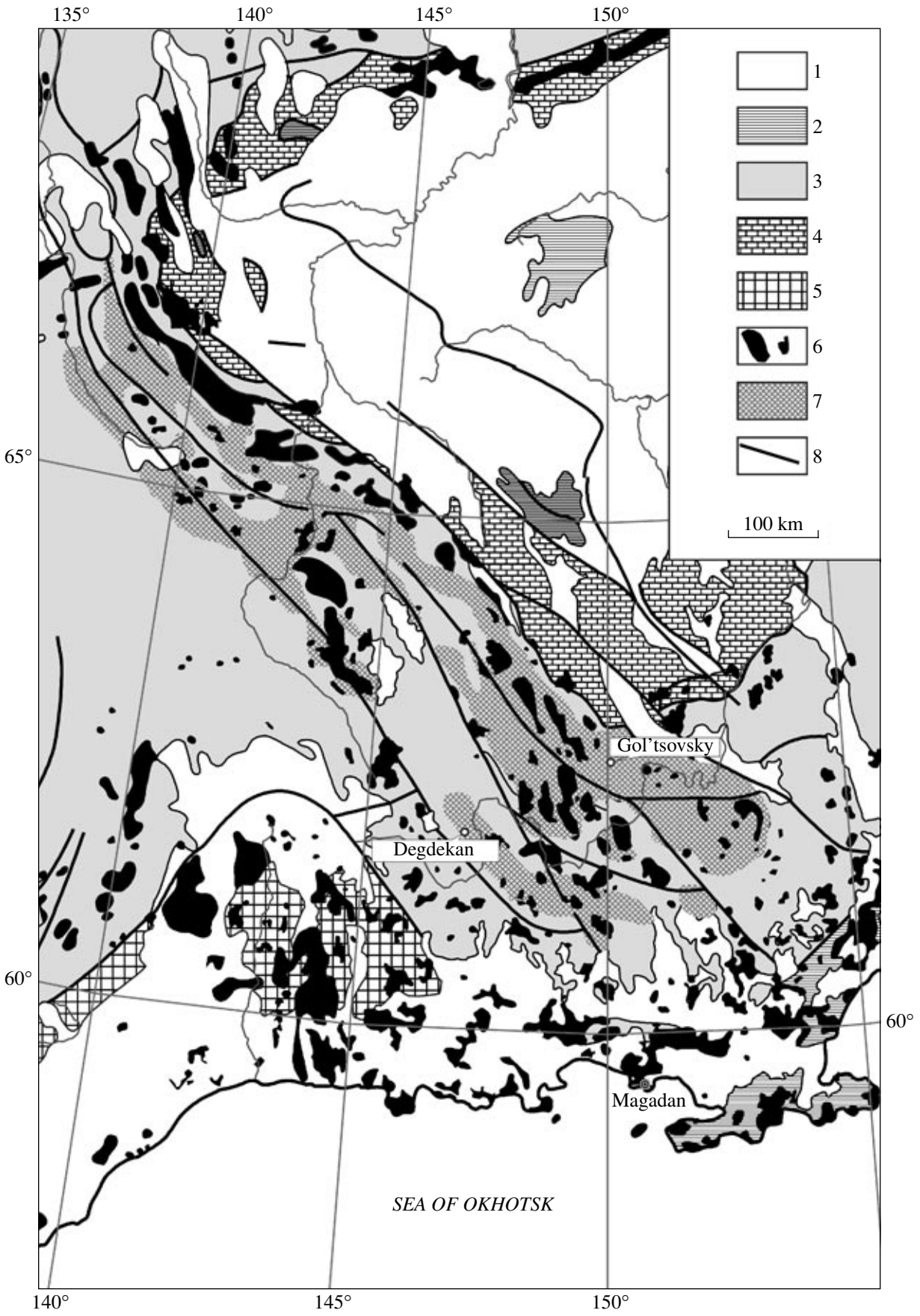
135°
140°
145°
150°
65°
60°
1
2
3
4
5
6
7
8
100 km
Gol'tsovsky
Degdekan
Magadan
SEA OF OKHOTSK
140°
145°
150°
60°

tonic turbidite terranes, and the Polousny–Debin Terrane of the turbidite accretionary wedge (*Tectonics...*, 2001).

The Degdekan deposit is located in the basin of the creek bearing the same name and is hosted in the Permian terrigenous rocks of the Ayan–Yuryakh Anticlinorium, being controlled by the Tenke Fault Zone. The host rocks are Upper Permian monotonous mudstones and siltstones about 2.5 km thick. The terrigenous rocks are metamorphosed under greenschist facies conditions and cut through by a linear swarm of Late Mesozoic acid and intermediate dikes trending W–E conformably to the host rocks (Fig. 2). The earliest andesite and microdiorite minor intrusions are intramineral, acid dikes (dacites and rhyolites) are presumably postmineral, and spessartites were found to be definitely postmineral (Voroshin, 1988). The spessartite dikes are tens of meters long and a few meters thick. Their morphology, with offsets along lateral fractures, is the most complex. The postmineral spessartites contain numerous xenoliths of the basement rocks, including granite gneisses and garnet and biotite–garnet gneisses (Babaitsev, 1984).

At a distance from the contact with quartz veins, the rocks of postmineral dikes have a fine-grained texture made up mainly of green hornblende and plagioclase. On approaching the contact, the rocks acquire a porphyritic appearance. Hornblende phenocrysts are incorporated into the fine-grained pilotaxitic groundmass. The hornblende phenocrysts are replaced by a chlorite–carbonate aggregate with fine disseminations of ore minerals related to cleavage planes and crystal faces.

The orebodies are extended quartz veins conformable with the bedding of the host rocks, as well as mineralized zones and stringer–disseminated mineralization hosted in terrigenous rocks and dikes. Fifteen orebodies are recognized; orebodies 1/5 and 8 are the largest and contain more than 80% of gold reserves at the deposit.

Orebody 1/5 consists of two quartz veins located at the hanging contact (vein 1) and the lying contact (vein 5) of an albitized and carbonated microdiorite dike. The quartz veins crosscut the dike, on the one hand, and occur as xenoliths in the intrusive rock, on the other hand, indicating the intramineral emplacement of magma. The veins are more than 250 m long and 0.4–1.3 m wide; they strike 270°–290° W and dip at angles of 45°–75° to the north. The average Au grade is ~9 g/t.

Orebody 8 is a quartz vein divided into separate lenslike blocks. The vein strikes W–E and dips at angles of 40°–80° to the north conformably with the bedding of metaterrigenous rocks. The orebody is controlled by a bedding-plane detachment. The vein has a banded texture caused by coaly clay partings and linear arrangement of ore minerals and carbonates. The banded veins are occasionally dissected by transverse quartz veinlets. The vein extends for 1400 m along the strike and is traced for 240 m down the dip. The thickness varies from 0.1 to 2.1 m, attaining 4.5 m in swells. The average gold grade is ~4 g/t. A postmineral spessartite dike trends parallel to the vein over its entire extent. As seen in exposures and rock fragments, dike offsets crosscut the quartz vein.

Quartz, ankerite, and feldspar are the major gangue minerals, while arsenopyrite, pyrite, sphalerite, galena, chalcopyrite, and native gold are the most abundant ore minerals.

The Gol'tsovsky deposit is situated at the drainage divide between the Tumanny and Gol'tsovsky creeks in the upper reaches of the Malen'ky Creek and hosted in the flysch sequence of the In'yali–Debin Synclinorium, being controlled by the deep Middle Kan–Shturmovy Fault. It should be noted that the placer in the Maly Yuryakh River valley, where the Go'ltsovy Creek disembogues, is the second in amount of mined gold among the placer deposits of the Yana–Kolyma Belt (Voznesensky et al., 1999).

The gold mineralization is localized in Middle Jurassic siltstones and mudstones metamorphosed under greenschist facies conditions (Fig. 3). The host rocks are characterized by abundant large (up to 7–10 cm) star-shaped nodules of bituminous black calcite. Metaterrigenous rocks at the deposit are intruded by strongly altered intermediate and basic dikes with numerous offsets into gold–quartz veins. At the same time, separate quartz–carbonate veinlets intersect the dikes. Relics of the primary fine-grained structure are retained in dikes only occasionally. The primary minerals are commonly replaced by a quartz–feldspar–mica aggregate and strongly limonitized.

The orebodies are made up of quartz veins and sulfide–quartz stringer zones. The veins are 10–100 m long and 0.5–1 m (up to 3.5 m) thick; they strike NW conformably with fold axes (280°–310° NW) and steeply dip at angles of 80°–85° to the northeast and southwest. The sulfide–quartz stringer zones are as thick as 5 m and traced for a distance varying from 25 m to several hundred meters, revealing en echelon arrangement. The ore is brecciated, massive, or banded. The master veins at the Gol'tsovsky deposit were named (Fig. 4). In the unmetamorphosed ore, the gangue minerals are quartz, albite, ankerite, calcite, and

Fig. 1. Location of the Degdekan and Gol'tsovsky deposits in the Yana–Kolyma gold belt. The tectonic base was compiled after Greninger et al. (1999). The belt is bounded by fields of placers and ore occurrences (Shilo, 1960). (1) Upper Jurassic–Quaternary volcanosedimentary cover, unspecified; (2) island arc terranes and fragments of the oceanic crust; (3) metaturbidites of the Verkhoyansky Fold–Thrust Belt and the Kular–Nera, Viliga, and Polousny–Debin terranes; (4) terranes of the passive continental margin, unspecified; (5) cratonic Okhotsk Terrane; (6) unspecified granitoids; (7) Yana–Kolyma gold belt; (8) faults.

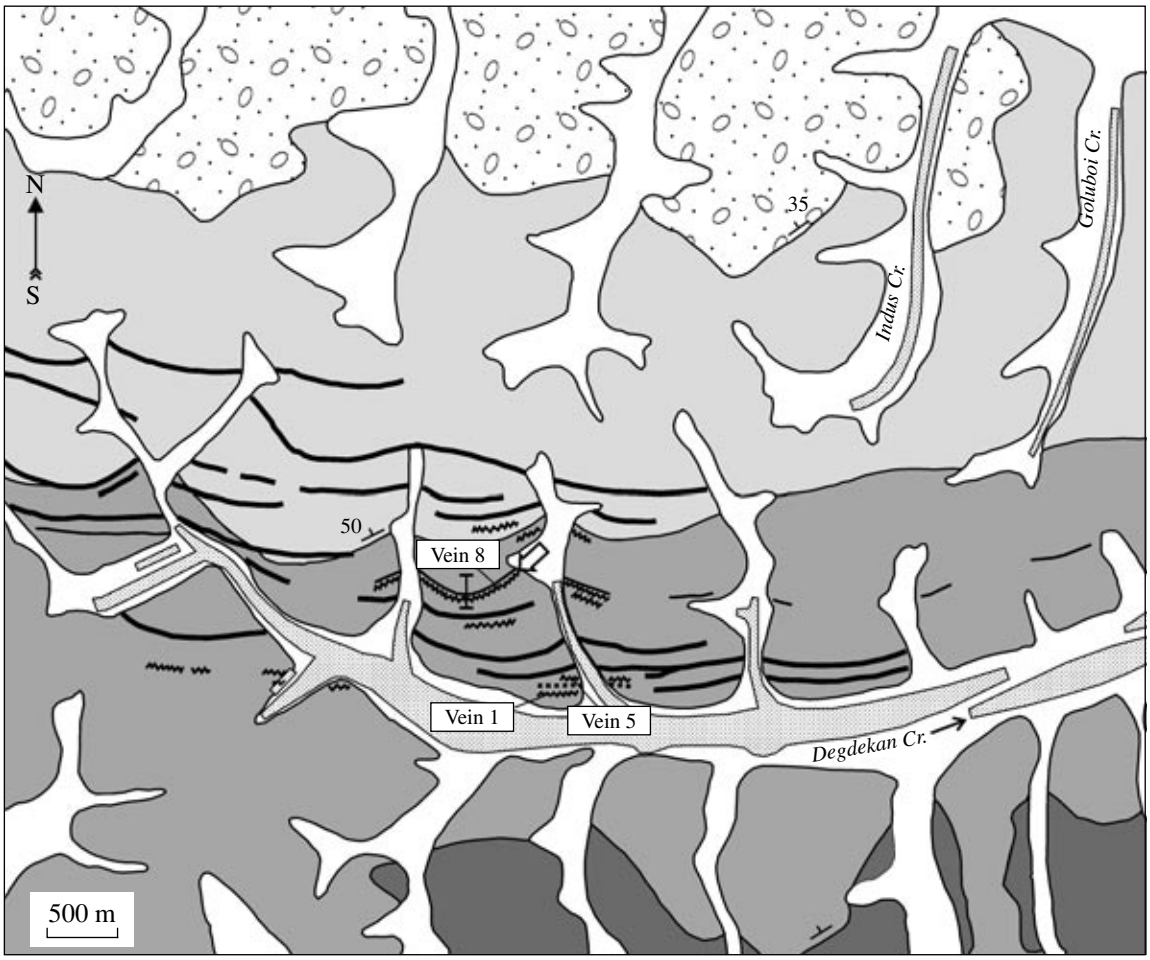
N
S
35
Indus Cr.
Goluboi Cr.
50
Vein 8
Vein 1
Vein 5
Degdekan Cr.
500 m

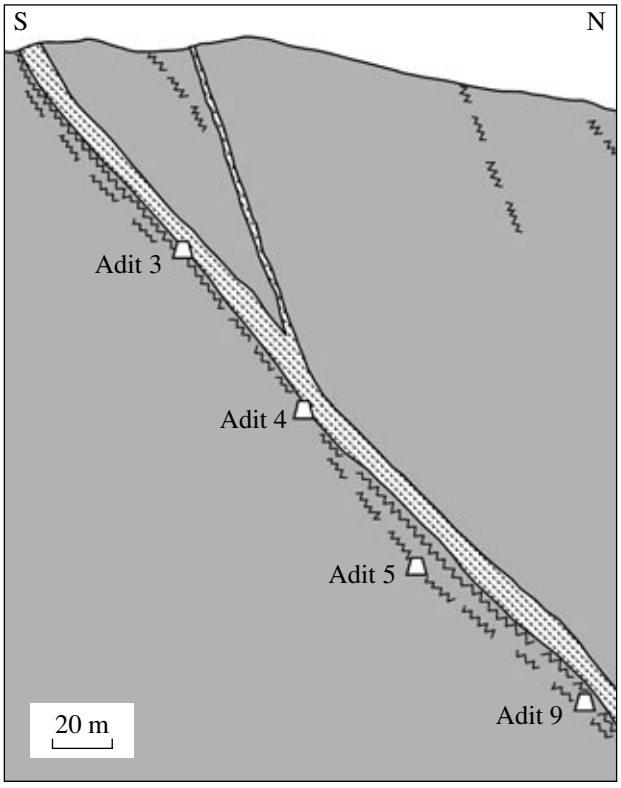
S
N
Adit 3
Adit 4
Adit 5
Adit 9
20 m

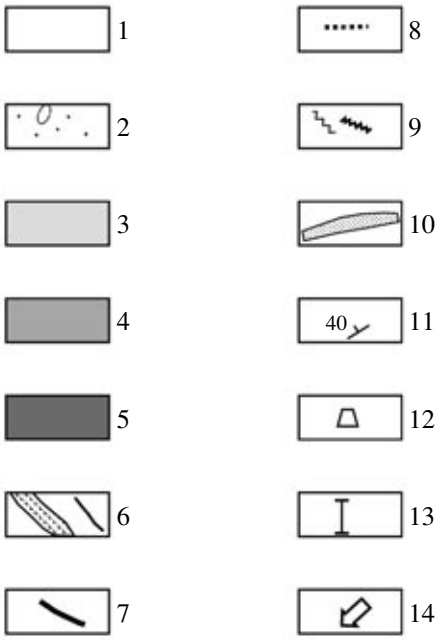
1
2
3
4
5
6
7
8
9
10
40
11
12
13
14

Fig. 2. Geological map of the Degdekan deposit and section across vein 8, modified after G.M. Shlyapnikov (1956) and Yu.P. Karelin et al. (1991). (1) Quaternary sediments; (2) diamictite of the Upper Permian Atkan Formation; (3) siltstone and mudstone of the Upper Pionersky Subformation, Upper Permian; (4) mudstone of the Lower Pionersky Subformation, Upper Permian; (5) flyschoid rocks of the Rodionov Formation, Lower Permian; (6) postmineral spessartite; (7) granite porphyry and rhyolite; (8) intramineral microdiorite; (9) quartz vein; (10) contour of placers; (11) dip and strike of rocks; (12) adit location; (13) section line in plan; (14) location of samples from the metamorphosed veins.

chlorite, while arsenopyrite, pyrite, sphalerite, galena, chalcopyrite, and native gold are ore minerals.

RESEARCH METHODS

Unmetamorphosed quartz veins and mineral assemblages were studied in different areas of the Degdekan and Gol'tsovsky deposits at a significant distance from dikes to avoid their effect. Metamorphosed material was taken from the dumps of exploration underground workings (mine 3, adits 6, 7) along vein 8 at the Degdekan deposit, as well as from an exposure at the mouth of adit 6, where quartz is cut by a spessartite dike (Fig. 2). The contact metamorphism of a dike at the Gol'tsovsky deposit was studied in samples taken from trench 6, within the Linzochka and Preryvisty lenses, where vein quartz is crosscut by dikes of pervasively altered amygdaloidal basalts (Fig. 4).

The products of metamorphism were studied in thin and polished sections, as well as in polished plates, which were prepared from samples with welded dike–vein contacts. To extract disseminated sulfides, thin plates were cut from veins at different distances from the contact and then dissolved in HF. Afterwards, sul-

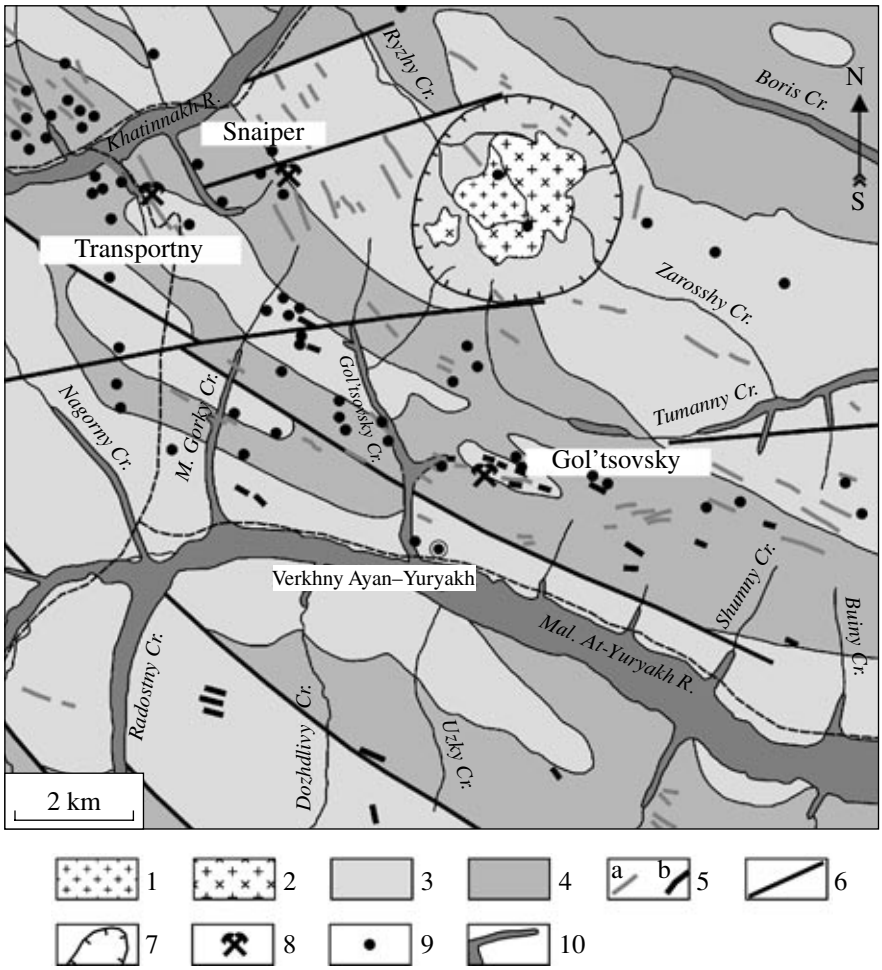

Fig. 3. Geological scheme of the Gol'tsovsky deposit, modified after O.P. Storozhuk et al. (1976). (1) Late Jurassic biotite granite; (2) Late Jurassic hornblende–biotite granodiorite; (3) siltstone-dominated flyschoid rocks of the Middle Jurassic Morzhovsky Formation; (4) mudstone-dominated flyschoid rocks of the Lower Jurassic Byuchennakh Formation; (5) unspecified dikes (a) and quartz veins (b); (6) faults; (7) biotite isograde; (8) Au deposits and occurrences; (9) showings of Au mineralizations; (10) contours of Au placers.

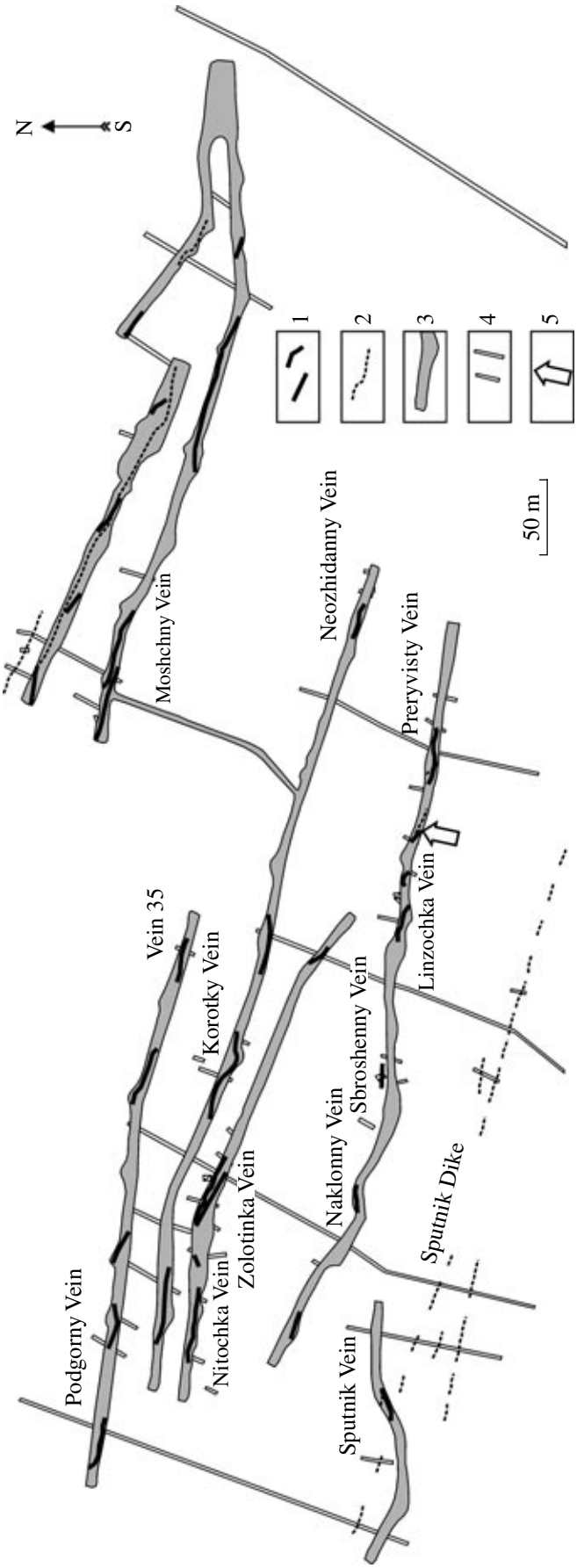

Fig. 4. Gold veins at the Gol'tsovsky deposit after A.E. Chicherin and S.P. Govorov (1984). (1) Quartz veins and veinlets; (2) dikes; (3) trenches driven in 1980–1981; (4) trenches driven prior to 1980; (5) location of samples from metamorphosed veins.

Table 1. Mineral composition of the Degdekan and Gol'tsovsky deposits

Mineral	Degdekan deposit		Gol'tsovsky deposi	
	unmetamorphosed veins	newly formed and regenerated minerals	unmetamorphosed veins	newly formed and regenerated minerals
Quartz	X	x	X	x
Ankerite	X	–	o	–
Calcite	o	o	o	o
Dolomite	o	–	–	–
Albite	x	–	x	–
White micas	o	–	o	–
Chlorite	o	–	o	–
Pyrite	X	o	X	o
Pyrrhotite	o	x	o	o
Arsenopyrite	X	x	X	x
Loellingite	–	x	–	–
Co–Ni sulfoarsenides	o	–	o	–
Sphalerite	X	x	o	–
Galena	X	x	o	–
Chalcopyrite	x	–	o	–
Tetrahedrite	o	–	–	–
Tennantite	–	o	–	–
Gold	x	o	x	–
Electrum	x	o	–	–
Scheelite	o	–	–	–
Apatite	o	–	o	–
Rutile	o	–	o	–

Note: Abundance of minerals: (X) major; (x) ubiquitous; (o) sporadic; a dash denotes not detected.

fides and their intergrowths were handpicked under a binocular microscope and mounted in pellets. Studied in most detail were sulfides of variable composition (arsenopyrite, sphalerite); native gold; and quartz, the major gangue mineral.

Sulfides and native gold were analyzed on a Camebax SX-50 microprobe (analyst G.A. Merkulov) at an accelerating voltage of 20 kV, an ion current of 30 nA, and a counting time of 5 s. The following analytical lines were used: K_α for Fe, As, S, and Zn; L_α for Ag; and M_α for Au. The standards included Asp200 (provided by S.D. Scott) and synthetic ZnS, FeS_2, and Au–Ag alloys. Each grain was analyzed at one or two points. Particular minerals were examined by profile scanning. Analyses with totals of 100 ± 1.5 wt % were selected to plot histograms. The trace element contents were determined selectively by chemical, spectral, and microprobe analyses.

Sixty-five double-polished quartz plates were examined and 16 of them were taken for thermometric analyses of individual fluid inclusions. Thermo- and cryometric studies of fluid inclusions were performed on microthermo- and cryostages constructed by Osorgin and Tomilenko (1990a, 1990b). The accuracy of thermometric measurements was controlled by systematic calibration of the stages using standard fluid inclusions and synthetic materials with known melting and freezing temperatures. The investigations were conducted with a measurement accuracy of ±0.1°C within the temperature interval from +31 to –150°C and with an accuracy of ±5°C in the temperature interval from +100 to +700°C. The concentration and salt composition of the aqueous phase of fluid inclusions were studied by cryometric measurements from the ice melting temperature in the NaCl–H_2O system (Kirgintsev et al., 1972; Borisenko, 1977; Roedder, 1984). The pressure of mineral-forming fluids was determined from the *PVT* diagram for the CO_2–H_2O system using the isochore and isotherm intersection for a pair of syngenetic carbon dioxide and aqueous inclusions (Roedder and Bodnar, 1980; Kalyuzhny, 1982). The isotherm was determined from the homogenization temperature of aqueous solutions, and the isochore, through CO_2 density using the partial homogenization temperature of carbon dioxide inclusions. The fluid pressure was calculated with the

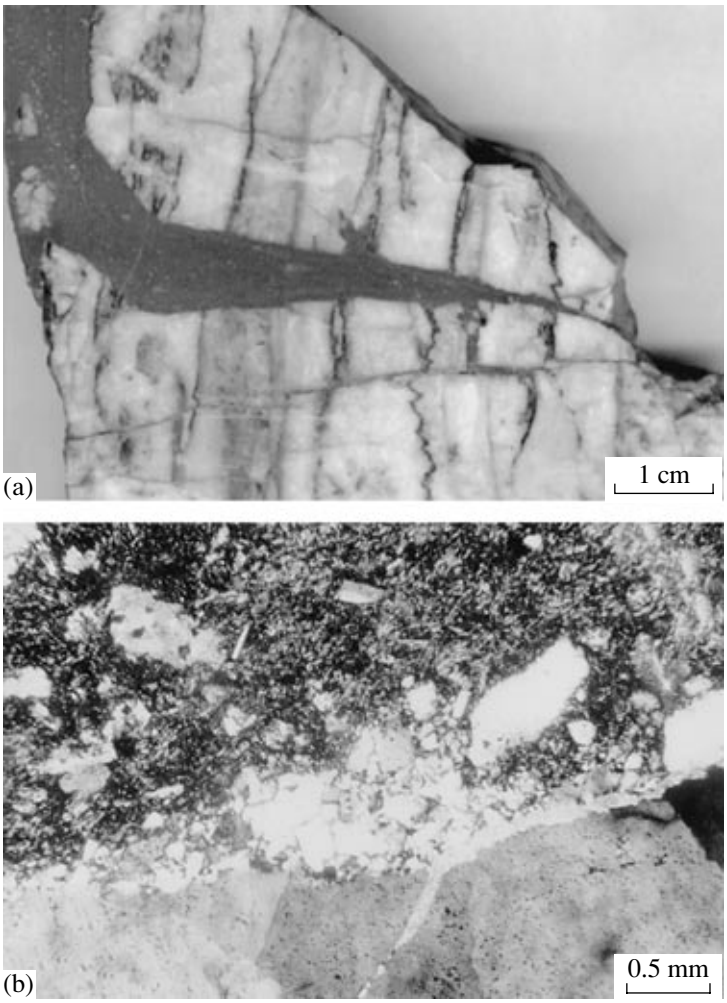

Fig. 5. Relationships of dike and quartz vein at the Degdekan deposit. (a) Offsets of spessartite dike (dark gray) crosscut the banded quartz vein; (b) granulation of quartz along the contact with the dike. Microphotograph without analyzer.

program FLINCOR (Brown, 1989; Brown and Hagemann, 1994). The results obtained are highly similar to the pressure estimates based on the *PVT* diagrams.

The chromatographic analysis of gases was carried out on an assembly consisting of three unmodified LKhM-80 chromatographs and having an original device for thermal and mechanical extraction of gases (Osorgin, 1990). Quartz grains 0.5–0.25 mm in size devoid of mineral inclusions were handpicked under a binocular microscope. The samples picked were treated with low concentrations of HCl and HNO_3, washed in distilled water, and dried at a temperature of 105°C.

RESULTS

General Characteristics of Contact Alteration

Both deposits contain hydrothermal mineralization of the same type (Table 1). Sphalerite and galena as equant and interstitial disseminated grains in quartz are ubiquitous minerals at the Degdekan deposit. They also form intergrowths with pyrite, arsenopyrite, or native gold no more than a few millimeters in size. Arsenopyrite and pyrite are major sulfides at the Gol'tsovsky deposit. The former occurs as large (up to a few centimeters in size) crystalline or nodular aggregates in quartz and as scarce small euhedral crystals disseminated in the wall rocks. The bulk of ore minerals are observed in selvages of quartz veins or in fragments of terrigenous rocks incorporated into quartz. The total amount of sulfides is no more than a few percent, typically less than 1%.

Quartz at the contact with spessartite at the Degdekan deposit is visually indistinguishable from quartz located at a distance from igneous bodies, only occasionally acquiring a specific tint, presumably owing to recrystallization. The contact is commonly conformable to the vein banding, giving the impression that it was formed in cavities of spalling along the cooled intrusion. However, the very thin fissures in quartz veins filled with spessartite point to penetration of magmatic melt that led to tearing off and cementing of quartz fragments (Fig. 5a). Occasionally, the breccia-

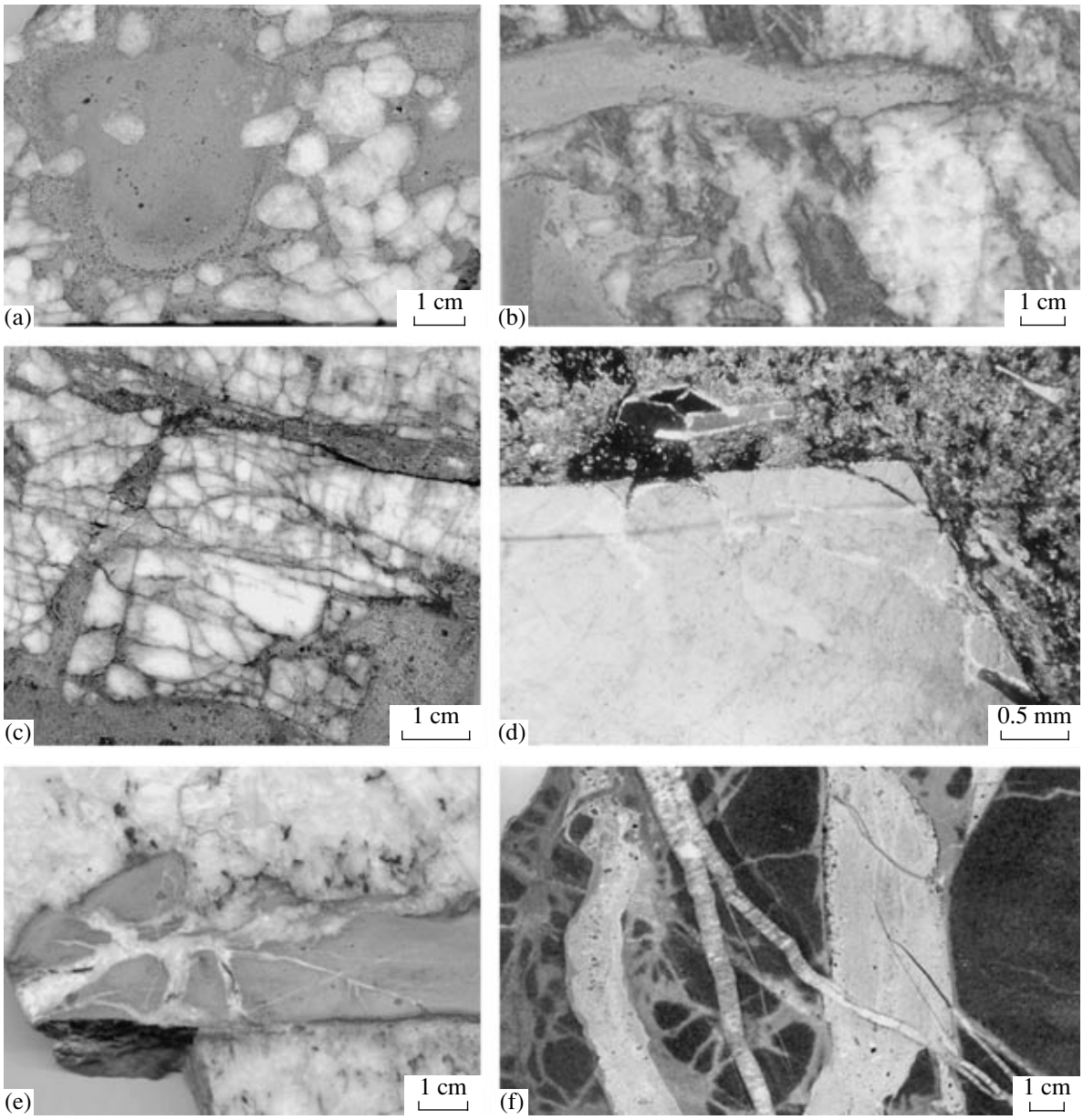

Fig. 6. Relationships of dike and hydrothermal rocks at the Gol'tsovsky deposit. (a) Dike (gray) cements quartz grains regenerated into euhedral crystals; (b) brecciated quartz vein is crosscut by a dike offset (light gray); (c) cataclastic quartz is crosscut by dike offsets (gray); (d) contact between euhedral quartz and cementing dike (close-up of Fig. 6a); quartz is not granulated; (e) quartz–feldspar "pseudoveinlets" in a dike offset; (f) dike (light gray) is crosscut by thin quartz–carbonate veinlets.

tion of vein material may be observed along the contact. Microscopic examination showed that quartz in small fragments is recrystallized from a medium- to a fine-grained aggregate as was described by Firsov (1956, 1958) in veins at the contacts of granitoid massifs.

At the Gol'tsovsky deposit, the vein segments that come into contact with dikes experienced more obvious alteration under effect of magmatic melt. It is seen that the granular gangue quartz was recrystallized into individual crystals, which are completely embedded in magmatic material or have their tops directed toward the melt (Fig. 6a). However, in many cases, quartz grains are not enlarged or faceted during the emplacement of intrusions, even when the melt penetrates into highly cataclastic quartz (Figs. 6b, 6c). There is also no evidence of granulation, which is typical of metamorphosed quartz at the Degdekan deposit (Fig. 6d).

Fragments of quartz with arsenopyrite pockets were found in amygdaloidal basalts crosscutting quartz veins at the Gol'tsovsky deposit (Fig. 7a). Arsenopyrite devoid of a quartz envelope was recrystallized to form a fine-grained aggregate of sheathlike crystals with rhombic sections. In partly mantled arsenopyrite, recrystallization develops only locally or along frac-

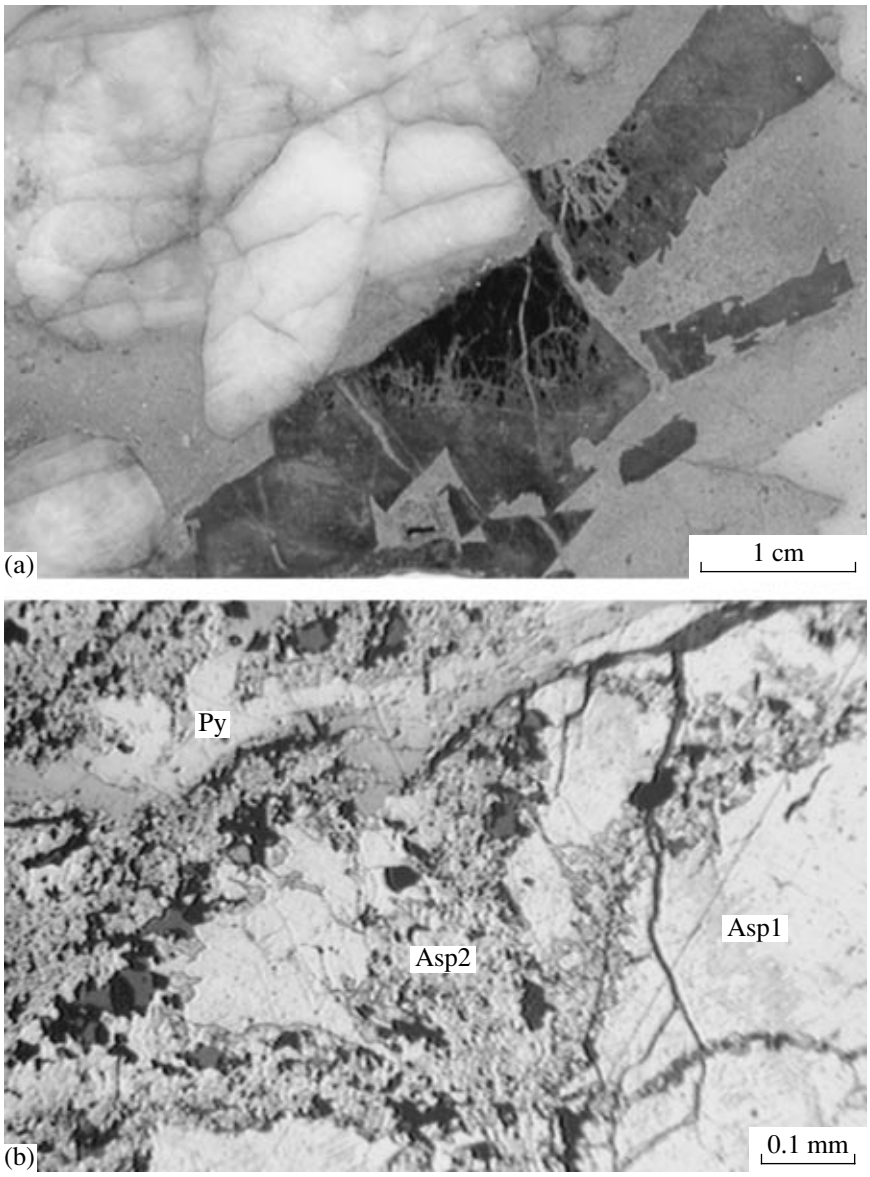

Fig. 7. Metamorphism of sulfides at the Gol'tsovsky deposit. (a) Dike (light gray) serves as a cement for arsenopyrite (dark gray) and quartz (white); (b) recrystallization of primary (nonmetamorphosed) arsenopyrite (Asp1) into fine-grained arsenopyrite (Asp2) and pyrite (Py) (close-up of Fig. 7a). Polished section. Microphotograph without analyzer.

tures, forming specific veinlets. On the side of quartz-protected margin, the pockets are overgrown by pyrite or cut by lenslike pyrite veinlets, which intersect both the massive primary arsenopyrite and its recrystallized aggregate (Fig. 7b). Note that pyrrhotite and loellingite, the typical alteration products of arsenopyrite in the near-contact zones of the spessartite dikes at the Degdekan deposit, were not found here.

Ore Minerals

Arsenopyrite in quartz veins, veinlets, and products of wall-rock alteration at a distance from contact with postmineral dikes makes up euhedral equant, flattened, or long prismatic crystals from fractions of a millimeter to a centimeter in size (Fig. 8a). The quartz veins at the Gol'tsovsky deposit commonly contain nodules of coarse-grained arsenopyrite attaining a few centimeters in size. The etching of polished thin sections reveals a finely or blockily zoned internal structure without a distinct zonal distribution of major and trace elements. The arsenopyrite composition does not depend on the assemblage of minerals in microintergrowths. The content of trace elements (Co + Ni + Mo) does not exceed 0.5 at %. The As and S contents in arsenopyrite from the unmetamorphosed quartz veins at both deposits show a nearly normal distribution (Figs. 9a, 9b). The As contents in the unmetamorphosed arsenopyrite at the

Degdekan deposit vary from 29 to 32.5 at % (31.2 at % on average; standard deviation is 0.7; $N = 252$); those at the Gol'tsovsky deposit vary within a similar range, from 29.5 to 33 at % (31.2 at % on average; standard deviation is 0.7; $N = 50$). All calculations were performed at a 95% confidence level.

Arsenopyrite from quartz veins at the contact with dikes at the Degdekan deposit was found to comprise fine-grained irregular aggregates in close intergrowths with pyrite, pyrrhotite, loellingite, and occasionally sphalerite and galena. These aggregates often form pseudomorphs after the primary arsenopyrite (Figs. 8b, 8c). The As content in arsenopyrite from metamorphosed samples at the Degdekan deposit varies from 29 to 40 at % ($N = 142$; Fig. 9c). The highest As contents were presumably caused by the occurrence of loellingite microinclusions.

The recrystallized fine-grained arsenopyrite in large aggregates entrapped by a dike at the Gol'tsovsky deposit exhibits only an insignificant increase in As content (Fig. 9d), which is within the range 30–33.5 at % (31.8 at % on average; standard deviation is 0.8; $N = 16$). The statistical *t*-test showed that there are no significant differences in the average As contents between the unmetamorphosed and the metamorphosed arsenopyrite.

Pyrite at both deposits occurs as abundant disseminations of small (tenths of a millimeter) crystals with relics of globular texture hosted in metaterrigenous rocks or as crystalline segregations in carbonate nodules. Pyrite in the altered wall rocks is recrystallized; the grains are increased in size and often contain small (0.0*n* mm) inclusions of the cobaltite–gersdorffite series, pyrrhotite, sphalerite, and galena. Pyrite from sedimentary rocks typically contains (wt %) 46.5 Fe, 51.8 S, and 0.8 As.

Pyrite occurs in quartz as small discrete grains and their aggregates or intergrowths with arsenopyrite, galena, and sphalerite. Near the contacts of dikes at the Degdekan deposit, pyrite was found only in fine-grained intergrowths with pyrrhotite, arsenopyrite, and loellingite. At the Gol'tsovsky deposit, rims of crystalline pyrite around aggregates of recrystallized arsenopyrite were detected at a distance of a few millimeters from the contact. The As content in pyrite from the contact zones varies from 0 to 6.2 wt %. The poor reproducibility of the analyses may be attributed to the involvement of arsenopyrite microinclusions by the microprobe beam. Within a few millimeters from the contact with a dike, pyrite is occasionally transformed into pyrrhotite, which, in turn, is replaced by a marcasite–pyrite aggregate. The dikes themselves at both the Degdekan and the Gol'tsovsky deposits contain finely disseminated cubic pyrite, which was presumably produced by retrograde metamorphic reactions.

Cobalt and nickel sulfoarsenides were detected as microcrystalline inclusions in pyrite in the outer zones of wall-rock alteration. They are of variable composition, but the size of the inclusions is often too small to permit quantitative analysis. The sulfoarsenides did not undergo metamorphism.

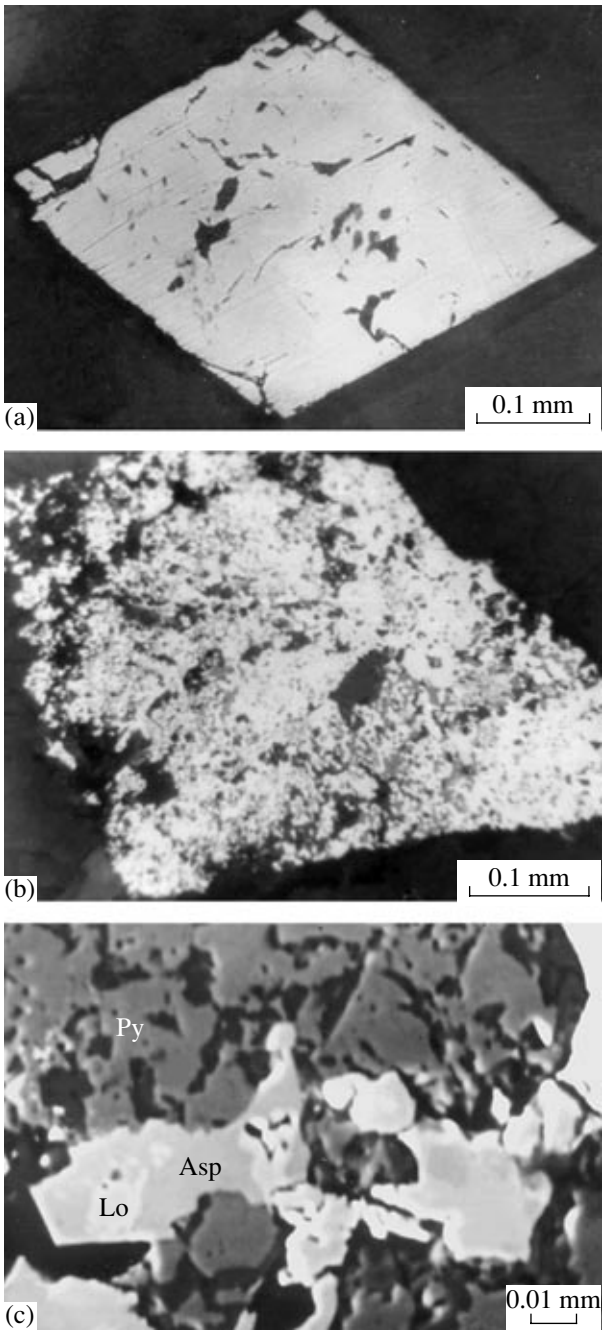

Fig. 8. Metamorphism of sulfides at the Degdekan deposit. Polished sections. (a) Typical euhedral crystal of unmetamorphosed arsenopyrite; (b) fine-grained pseudomorphs of arsenopyrite (Asp), loellingite (Lo), pyrite (Py), and pyrrhotite (Po) after the primary arsenopyrite; (c) close-up of Fig. 8b (image in absorbed electrons).

Loellingite at the Degdekan deposit was detected only at the contact with dikes in the aforementioned fine-grained intergrowths with pyrite, pyrrhotite, and arsenopyrite (Fig. 8c).

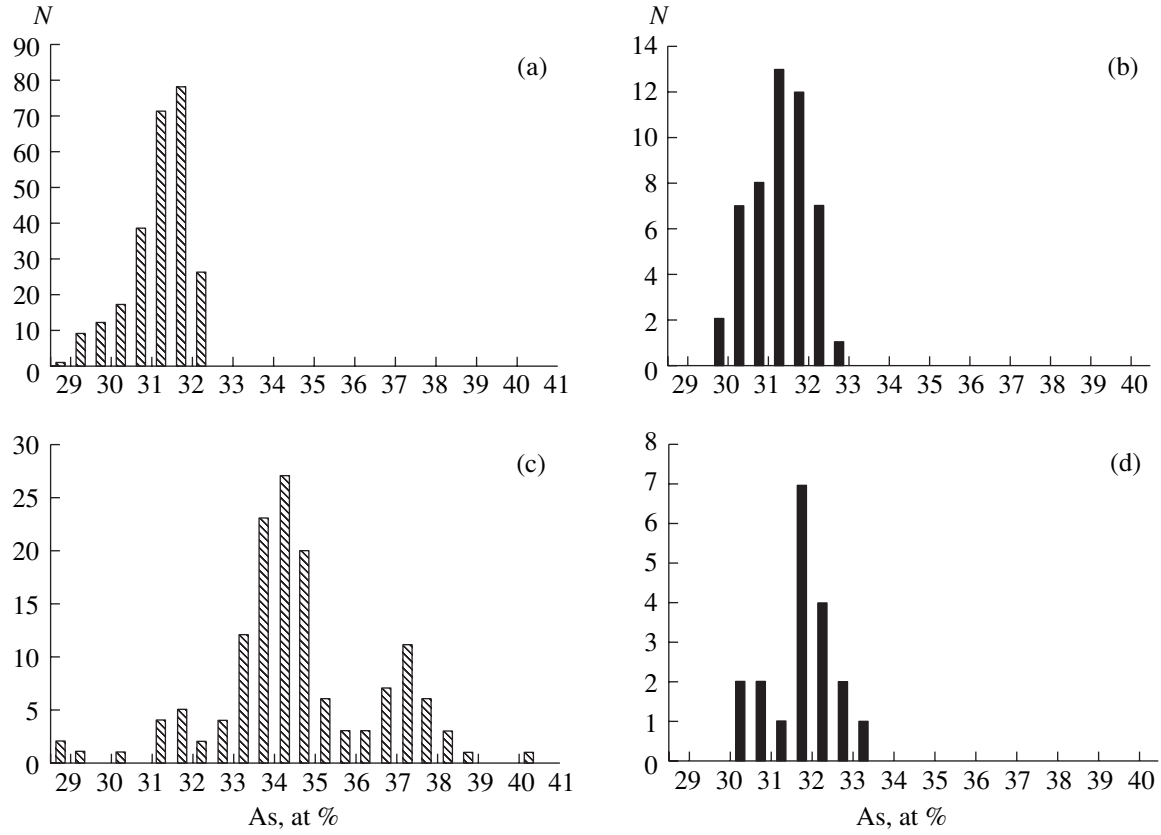

Fig. 9. Compositional variations in arsenopyrite from the Degdekan (a, c) and Gol'tsovsky (b, d) deposits. (a, b) Unmetamorphosed veins; (c, d) metamorphosed veins.

Pyrrhotite appears as very fine, presumably syngenetic inclusions in pyrite metacrysts hosted in sedimentary rocks; pyrrhotite contains 59.6 wt % Fe and 39.9 wt % S. Newly formed pyrrhotite was also identified in the vein segments affected by contact metamorphism. At the Degdekan deposit, it occurs in the polymineral intergrowths described above and as sporadic pseudomorphs after pyrite, which, in turn, are often replaced by characteristic marcasite–pyrite aggregates. At the Gol'tsovsky deposit, no newly formed pyrrhotite was found in quartz veins near the dike contacts.

Sphalerite was studied in the ore of the Degdekan deposit. At the Gol'tsovsky deposit, where this mineral is significantly less abundant, it was not identified in the metamorphosed rocks. Sphalerite in quartz veins at a distance from dikes occurs as pale yellow or light brown equant grains less than 1 mm across. The mineral is always impregnated with chalcopyrite emulsion. Compositional variations in sphalerite from intergrowths with other Fe-bearing sulfides explain the asymmetric distribution of FeS in this mineral (Fig. 10a). The Fe contents in sphalerite vary from tenths to 7 at %, being 2.4 at % on average (standard deviation is 1.12; $N = 147$). The Cd + Mn content is no higher than 0.5 at %. The formation temperature of sphalerite-bearing assemblages in the unmetamorphosed veins at the Degdekan deposit was estimated from the sphalerite–galena sulfur isotope thermometer at 174 and 202°C (Voroshin and Eremin, 1995).

Sphalerite in quartz veins at contacts with dikes occurs as separate equant grains and close intergrowths with arsenopyrite, loellingite, pyrrhotite, and pyrite. The mineral is devoid of emulsion disseminations of chalcopyrite, and dark brown sphalerite grains appear. The Fe content shows notable variations (Fig. 10b). The lowest content of the troilite endmember was determined in the monomineral aggregates. High contents (14.3 at % Fe) were detected in the sphalerite intergrown with pyrrhotite, arsenopyrite, and loellingite, although they were also noted in separate grains. No correlation was established between the sphalerite composition and the distance from the contact with a dike.

Chalcopyrite in the primary ore was mainly identified as emulsion disseminations in sphalerite, which disappear in metamorphosed areas. In addition, chalcopyrite was established as fine-grained aggregates, ovoid segregations together with galena and sphalerite in sedimentary rocks, and syngenetic microinclusions in pyrite metacrysts.

Galena occurs in close intergrowths with sphalerite and does not show any specific features in metamorphosed areas.

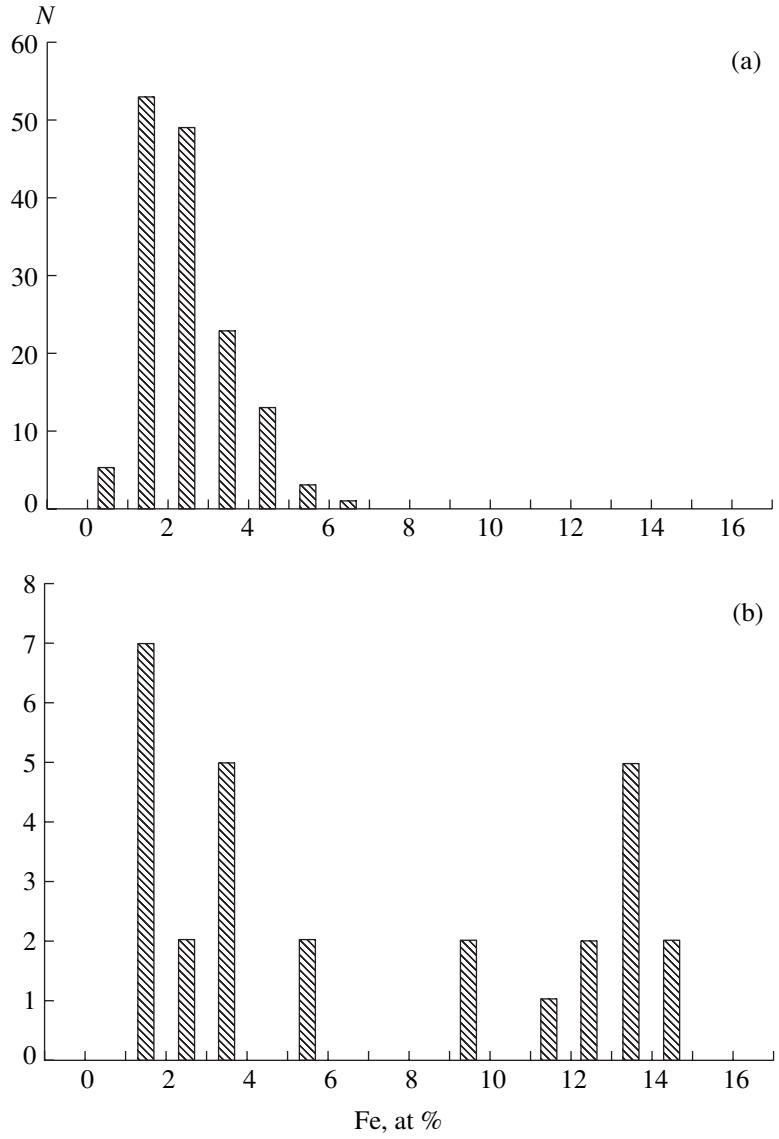

Fig. 10. Distribution of Fe in sphalerite from (a) unmetamorphosed and (b) metamorphosed quartz veins at the Degdekan deposit.

Tennantite–tetrahedrite is observed as small inclusions in arsenopyrite metacrysts from altered wall rocks at the Degdekan deposit. The mineral has the following composition (wt %): 37.8 Cu, 3.6 Fe, 5.5 Zn, 12.1 As, 14.4 Sb, and 26.3 S. In proximity to contact with a dike at this deposit, tennantite as a reaction mineral occurs at the grain boundary between arsenopyrite and sphalerite (Fig. 11) and has the following composition (wt %): 0.9 Ag, 42.5 Cu, 4.9 Fe, 5.0 Zn, 0.3 Sb, 19.8 Sb, and 27.7 S. The composition of associated sphalerite is (wt %) 63.3 Zn, 3.2 Fe, 0.3 Cu, and 32.0 S.

Native gold in the unmetamorphosed ore commonly occurs as interstitial irregular grains in quartz. Gold intergrows with galena and sphalerite and serves as a matrix for arsenopyrite and pyrite. At the contact with dikes, gold was studied only at the Degdekan deposit. The lumpy gold grains are smaller in size as compared to the gold from unaltered ore. Structural etching revealed a granular texture of gold aggregates. The metamorphosed gold is characterized by increased dispersion and an elevated absolute value of fineness that reaches 950 and is 890 on average (standard deviation is 57; $N = 26$). The fineness of unmetamorphosed gold exhibits a unimodal distribution and its average value is 790 (standard deviation is 18.8; $N = 186$) (Fig. 12). Pyrite and arsenopyrite metacrysts in the altered wall rocks contain small gold inclusions with a fineness of 620–680.

Fluid Inclusions in Quartz

Primary, pseudosecondary, and secondary fluid inclusions were recognized in quartz from unmetamorphosed and metamorphosed veins.

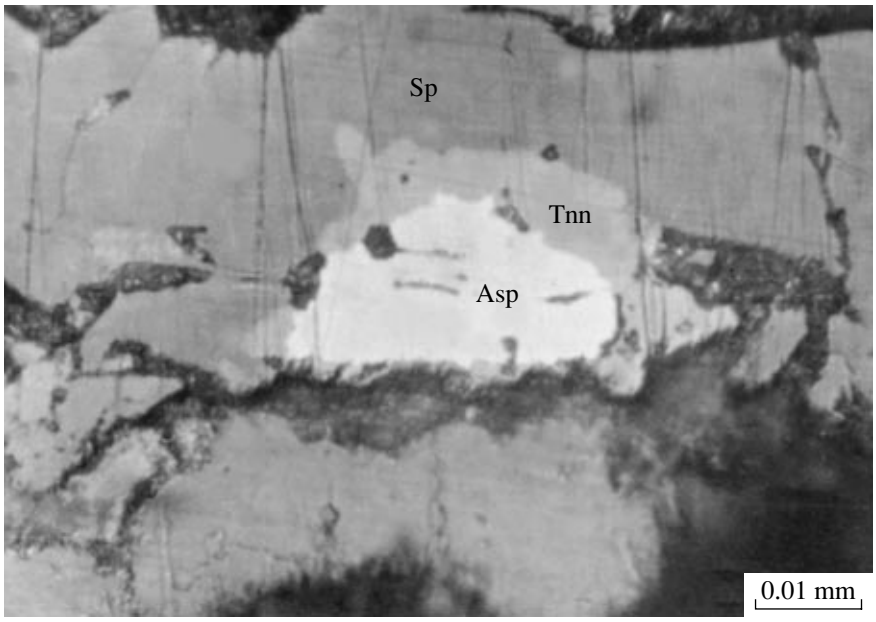

Fig. 11. Reaction rim of tennantite (Tnn) between arsenopyrite (Asp) and sphalerite (Sp). The Degdekan deposit. Polished section.

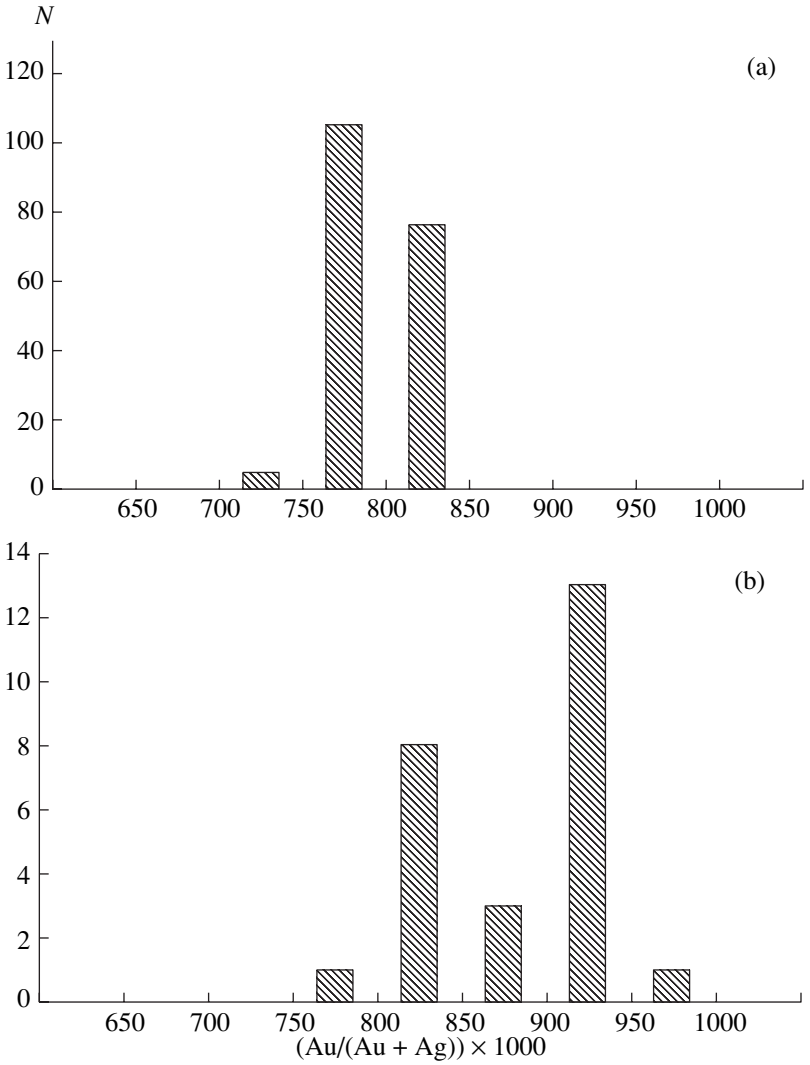

Fig. 12. Distribution of gold fineness in (a) unmetamorphosed and (b) metamorphosed quartz at the Degdekan deposit.

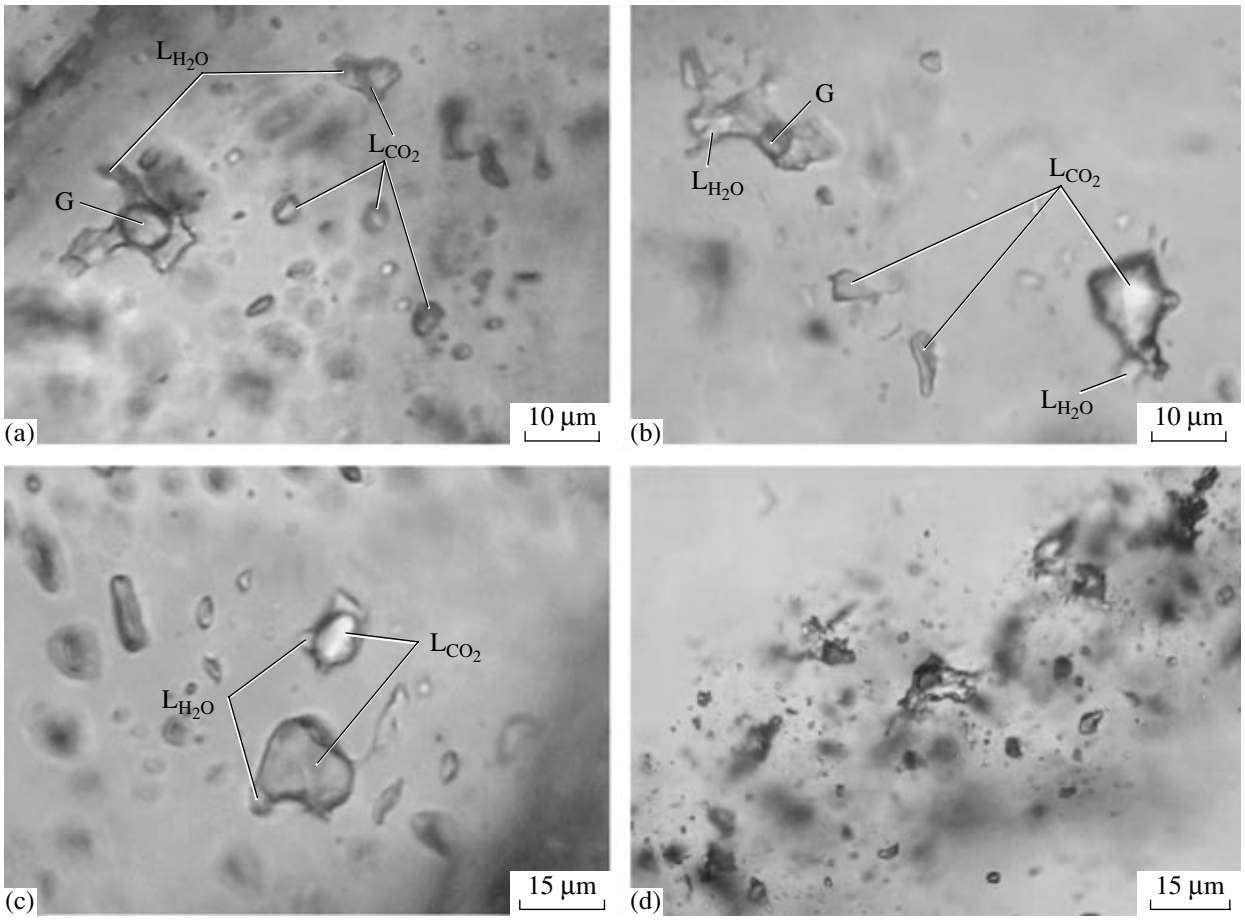

Fig. 13. Fluid inclusions in quartz from orebodies. (a, b) Aqueous and carbon dioxide fluid inclusions in unmetamorphosed quartz from the Gol'tsovsky deposit; (c) carbon dioxide inclusions in unmetamorphosed quartz from the Degdekan deposit; (d) decrepitated gas inclusions in metamorphosed quartz from the Degdekan deposit.

The primary inclusions, both individual and clustered, commonly form irregular or rounded vacuoles ranging in size from 5 to 10 (occasionally up to 15) μm.

The pseudosecondary inclusions are most typical. They appear as near-parallel discontinuous trails that do not cross the boundaries of quartz grains. The orientation of such trails differs from grain to grain. It is commonly assumed that the microcracks with discontinuous tracks of inclusions were induced by tectonic deformations during formation of quartz veins (Dugdale and Hageman, 2001). The pseudosecondary inclusions have a rounded elongated shape and vary in size from 10 to 15 μm.

The secondary inclusions are confined to the numerous microcracks that crosscut boundaries of quartz grains. They were found as rounded vacuoles from 1 to 5 (occasionally up to 10) μm in size. Owing to the small size, these inclusions were practically not studied.

The following types of fluid inclusions were recognized from microthermometric heating–cooling measurements: (1) aqueous (L_{H_2O} + G), (2) aqueous–carbon dioxide (L_{H_2O} + L_{CO_2} ± G), and (3) gas (G ± H_2O). The unmetamorphosed quartz veins contain only the two former types of fluid inclusions (Figs. 13a–13c). They occur jointly either as isolated groups or as separate trails that arose during crack sealing. The metamorphosed veins at the contact with dikes contain all three types of inclusions (Fig. 13d). The selective occurrence of gas inclusions close to the contacts with dikes gives grounds to suggest that they were formed as a result of partial or complete decrepitation of aqueous or carbon dioxide inclusions under the thermal effect of dikes.

Individual primary and pseudosecondary fluid inclusions in quartz were taken for microthermometric measurements. Their results are presented as histograms in Fig. 14 and Table 2. The low eutectic temperatures testify to the presence of Na, K, and possibly Mg chlorides in aqueous solution. The CO_2-bearing inclusions at both deposits have a higher ice melting temperature, ranging from –0.5 to –3.8°C, which corresponds to a salinity of 1–6 wt % NaCl equiv. The aqueous inclusions demonstrate a higher salinity of 6–14 wt % NaCl equiv., while T_{melt} varies from –3.8 to –9.3°C.

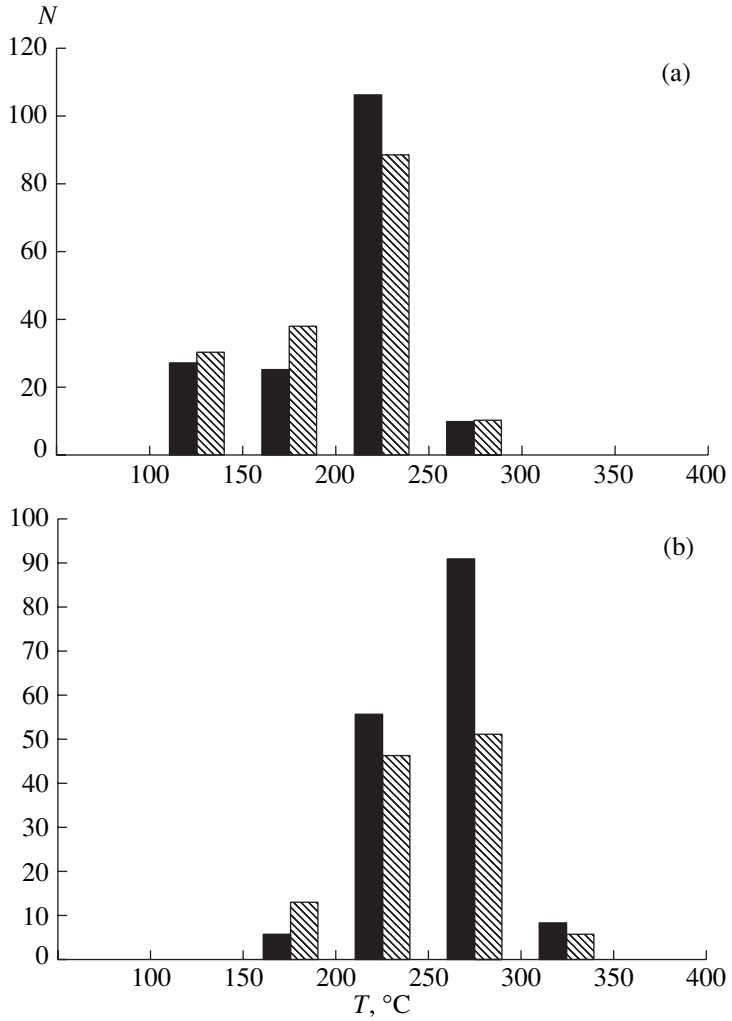

Fig. 14. Distribution of homogenization temperatures in (a) unmetamorphosed and (b) metamorphosed quartz from the Gol'tsovsky (black) and Degdekan (hatched) deposits.

The histograms show that the average homogenization temperature for primary and pseudosecondary inclusions is 206 ± 40°C (N = 334, confidence level is 95%) in quartz from unmetamorphosed veins and 257 ± 33°C (N = 277, confidence level is 95%) in quartz from metamorphosed veins. The salinity of the primary and pseudosecondary fluid inclusions in quartz from veins of both types varies from 0.5 to 14.0 wt % NaCl equiv. One can speak of an increase in fluid salinity in the inclusions from metamorphosed quartz.

The melting temperature of liquid CO_2 in the carbon dioxide inclusions varies from –57.0 to –60.8°C, indicating the presence of CH_4 and/or N_2 admixtures with lower melting temperatures than pure CO_2 ($T_{melt\ CO_2}$ = –56.6°C). In the carbon dioxide inclusions from unmetamorphosed quartz, CO_2 is homogenized into a liquid within the temperature range from +2.0 to +20.0°C, which accords with a fluid density ranging from 0.91 to 0.75 g/cm^3 (Vargaftik, 1972). In the metamorphosed veins, the temperature of CO_2 homogenization is shifted toward the low-temperature region and varies from –4.0 to +18.0°C (Fig. 15), which corresponds to the variation of fluid density from 0.95 to 0.77 g/cm^3.

The fluid pressure was determined from the *PVT* diagrams (Roedder and Bodnar, 1980; Kalyuzhny, 1982) using isochores of densities of carbon dioxide inclusions and homogenization temperatures of aqueous inclusions. The pressure of fluid entrapped in quartz of the unmetamorphosed veins varied from 0.7 to 1.3 kbar (T_{hom} = 180°C, density is 0.75 g/cm^3, and T_{hom} = 200°C, density is 0.91 g/cm^3, respectively). The fluid pressure in the inclusions in quartz from the near-contact zones is insignificantly shifted toward higher values of 0.8–1.5 kbar (T_{hom} = 200°C, density 0.77 g/cm^3, and T_{hom} = 220°C, density 0.95 g/cm^3, respectively).

Table 2. Results of microthermometric study of fluid inclusions in quartz from unmetamorphosed and metamorphosed veins at the Gol'tsovsky and Degdekan deposits

Deposit	Quartz	Sample	T_{hom}, °C	$T_{hom CO_2}$, °C	$T_{melt CO_2}$, °C	T_{eut}, °C	$T_{ice\ melt}$, °C	C_{salt}, wt % NaCl equiv
Gol'tsovsky	Unmetamorphosed	115/T-88	160–250	+2.5...+16	–58.1...–58.4	–23.4...–29.8	–1.5...–3.8	4–6
		126/T-88	145–260	+4.5...+12.6	–58.5...–60.2	–24.3...–28.7	–3.1...–9.3	5.5–14
		107/T-88	180–290	+5.2...+10.3	–58.5...–59.3	–23.4...–25.6	–0.5...–4.6	1–8.5
		135/T-88	180–275	+3.0...+10.2	–58.0...–59.2	–20.0...–23.5	–2.2...–5.3	5–9.5
		147/T-88	125–160	–	–	–17.3...–22.8	–0.5...–1.3	1–3
	Metamorphosed	150/T-88	290–330	+5.3...+16.4	–58.7...–60.0	–19.5...–23.4	–2.3...–4.8	6–8.5
		145/T-88	190–260	+4.3...+18.6	–58.2...–59.3	–24.3...–26.5	–0.5...–3.2	1–6
		152/T-88	270–315	–3.5...+13.6	–57.8...–58.3	–25.4...–28.3	–2.3...–3.6	5–7
		151/T-88	230–285	–2.2...+4.3	–59.2...–60.8	–21.6...–27.9	–2.1...–4.8	5–8.5
		3120/C-88	190–300	+0.5...+8.3	–58.7...–59.8	–24.2...–26.8	–2.4...–5.3	5–9.5
Degdekan	Unmetamorphosed	18.10.4	125–270	+8.5...+19.0	–58.7...–59.2	–25.3...–27.9	–0.3...–1.9	0.5–4
		18.13.2	140–300	+9.0...+19.5	–58.1...–58.8	–23.2...–25.8	–1.5...–2.3	4–5.5
	Metamorphosed	1965/C-95	170–310	–3.2...+21.0	–57.0...–57.5	–21.8...–23.5	–2.2...–4.5	5–8.5
		1955/C-95	170–290	–3.8...+20.2	–57.2...–58.8	–	–	–
		1845/C-85	160–310	–0.9...+9.3	–58.7...–59.2	–	–	–
		692/Sh-79-1	220–320	+4.5...+16.3	–58.0...–59.6	–23.6...–28.1	–2.3...–5.0	5.5–9.0

Note: A dash denotes not obtained.

According to the results of gas chromatography, in addition to CO_2 and H_2O, N_2 and CH_4 are contained as volatiles in amounts no more than 1.2 and 2.8 mol %, respectively (Table 3). The average bulk content of volatiles in quartz from the metamorphosed veins is approximately 1.5–2 times lower than in the unmetamorphosed veins (Fig. 16). In some samples of heated quartz, the CO_2 content increases up to 15.4 mol % (Table 3).

DISCUSSION

The sulfide aggregates localized in direct contact with igneous rocks allowed us to estimate the thermal effect exerted by dikes on the ore. The appearance of pyrrhotite, loellingite, and tennantite, as well as the changes in the composition and microstructure of arsenopyrite, sphalerite, and native gold, is satisfactorily accounted for by the thermal effect of dikes on the ore. The comparison of the observed mineral assemblages with available experimental data makes it possible to determine the conditions of thermal metamorphism.

The pyrrhotite pseudomorphs after pyrite near the contact of dikes at the Degdekan deposit are suggested to be products of pyrite breakdown at ~743°C according to the reaction (Kullerud and Yoder, 1959)

$$2FeS_2 \longrightarrow 2FeS + S_{2\uparrow}.$$

If redox conditions corresponded to the C/CO_2 buffer, as is evident from the occurrence of organic matter and carbonates in the host rocks, the reaction could have proceeded at a temperature as low as 200°C (Hall, 1986). However, this buffer more likely affects the stability of diagenetic and metamorphic pyrite dispersed in terrigenous rocks than that of the pyrite encapsulated in quartz. Therefore, the temperature at the contact of dikes at the Degdekan deposit, in all probability, was higher than the upper stability limit of pyrite. Owing to the insignificant abundance of monomineral pyrite, individual pyrrhotite grains are also scarce. It should be noted that the dikes themselves contain disseminated pyrite rather than pyrrhotite. If the dikes contained a primary iron sulfide and crystallized at a temperature above 743°C, pyrrhotite should be stable. The pyrrhotite could have been transformed into pyrite by the subsequent retrograde metamorphic reaction with the participation of CO_2 and water (Hall, 1986)

$$8FeS + 5CO_2 + 2H_2O = 4FeS_2 + CH_4 + 4FeCO_3.$$

The poorly encapsulated pyrrhotite grains in quartz could have experienced the same transformation.

The recrystallization of monomineral arsenopyrite along with compositional changes and the formation of newly formed pyrite near the cracks and intergranular boundaries at the Gol'tsovsky deposit may be explained with aid of the *TX* phase diagram for the pyrite–loellingite join of the Fe–As–S system (Kozlov et al., 1986). During thermal metamorphism, the composition of arsenopyrite remained constant up to the Asp + Py equilibrium. When this equilibrium was reached, the

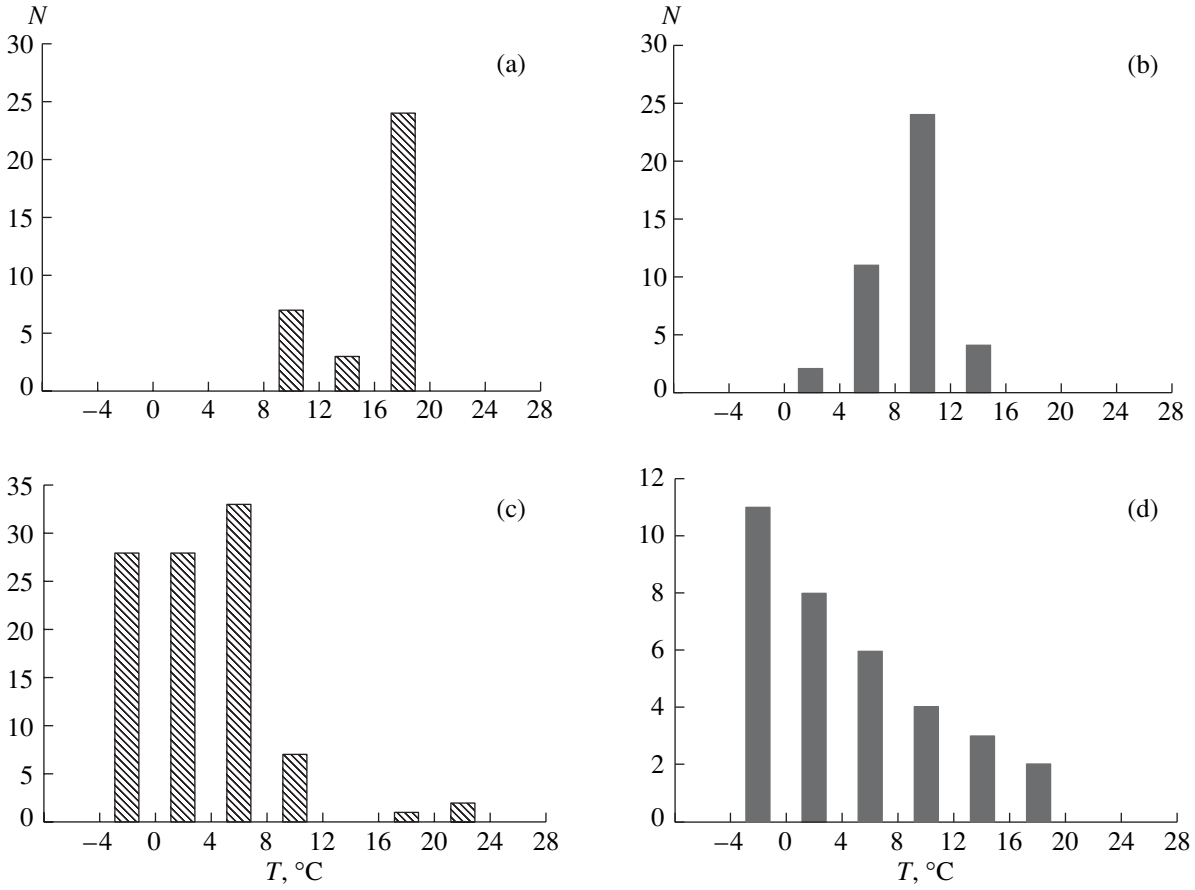

Fig. 15. Distribution of homogenization temperatures of CO_2 inclusions in (a, b) unmetamorphosed and (c, d) metamorphosed quartz from the (a, c) Degdekan and (b, d) Gol'tsovsky deposits.

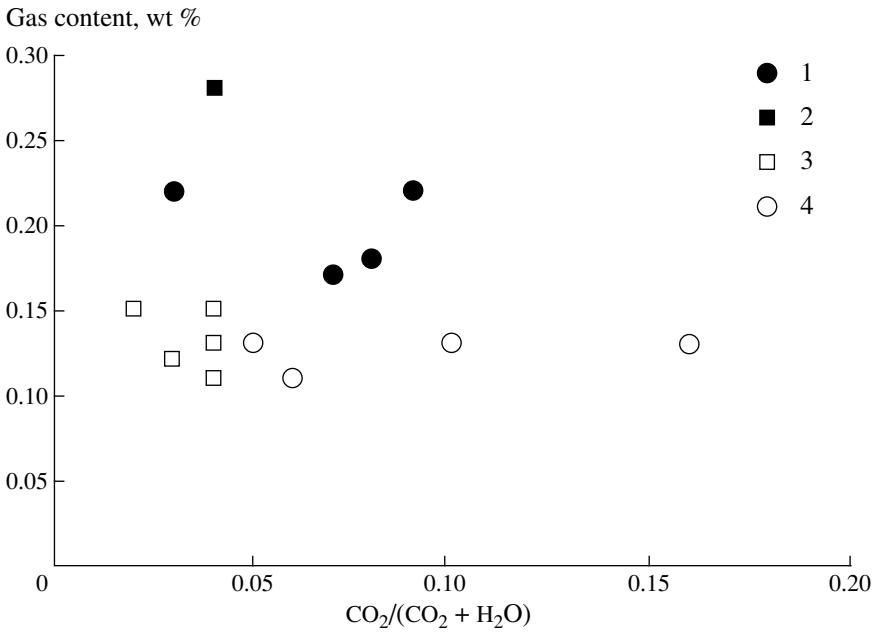

Fig. 16. Correlation between gas content and $CO_2/(CO_2 + H_2O)$ ratio in fluid from (1, 2) unmetamorphosed and (3, 4) metamorphosed quartz veins at the (2, 3) Degdekan and (1, 4) Gol'tsovsky deposits.

Table 3. Chemical composition of fluid inclusions in quartz from unmetamorphosed and metamorphosed veins of the Gol'tsovsky and Degdekan deposits (gas chromatography results)

Deposit	Quartz	Sample	Content, mol %				$CO_2/(CO_2 + H_2O)$	Gas content, wt %
			CO_2	H_2O	N_2	CH_4		
Gol'tsovsky	Unmetamorphosed	107/T-88	8.9	90.7	0.3	0.1	0.09	0.22
		115/T-88	2.8	96.8	0.3	0.1	0.03	0.22
		126/T-88	6.5	92.9	0.4	0.2	0.07	0.17
		135/T-88	7.5	91.8	0.5	0.2	0.08	0.18
	Metamorphosed	137/T-88	4.6	95.1	0.2	0.1	0.05	0.13
		151/T-88	5.6	94.0	0.3	0.1	0.06	0.11
		152/T-88	9.9	89.3	0.6	0.2	0.1	0.13
		3120/C-88	15.4	83.3	1.2	0.1	0.16	0.13
Degdekan	Unmetamorphosed	18.10.4	3.9	95.8	0.2	0.1	0.04	0.28
	Metamorphosed	18.8.22-1	4.3	95.5	0.0	0.2	0.04	0.11
		18.8.22-2	4.0	95.9	0.0	0.1	0.04	0.11
		1845/C-85	2.3	94.9	0.0	2.8	0.02	0.15
		420-9/B-80	2.9	97.0	0.0	0.1	0.03	0.12
		420-9/B-80a	3.7	96.1	0.0	0.2	0.04	0.15
		692/Sh-79-1	3.9	95.7	0.2	0.2	0.04	0.13
		692/Sh-79-2	3.9	95.7	0.3	0.1	0.04	0.13

Note: Temperature of gas release is 600°C; charge is 300 mg.

composition of arsenopyrite began to shift toward the As corner and pyrite started to precipitate, thus compensating a decrease in the S/As ratio in arsenopyrite. This phase composition is retained to a temperature of 491°C, at which pyrite and arsenopyrite are replaced by pyrrhotite + arsenopyrite (Clark, 1960). The absence of pyrrhotite at the Gol'tsovsky deposit indicates that the temperature at the contact of the dike was lower than 491°C. Unfortunately, a more accurate temperature estimate from the arsenopyrite geothermometer is hampered by a significant variation in the arsenopyrite composition, which may be explained by the nonequilibrium character of mineral assemblages that arose as a result of heating.

The intergrowths of loellingite, arsenopyrite, pyrrhotite, and pyrite and changes in the arsenopyrite composition at the Degdekan deposit serve as evidence for transformation during heating of arsenopyrite or pyrite–arsenopyrite assemblages. The phase proportions in newly formed assemblages depend on the initial proportions of pyrite and arsenopyrite, the duration and degree of heating, and the possibilities for removal of volatiles from intergrowths encapsulated in quartz. The sequence of arsenopyrite transformation by heating up to 491°C was shown above. During heating above this temperature, the composition of arsenopyrite in association with pyrrhotite should also be shifted toward the As corner, while a decrease in the S/As ratio in arsenopyrite should be compensated by the newly formed pyrrhotite. Arsenopyrite is transformed into loellingite + pyrrhotite at a temperature of 702°C (Clark, 1960). This entire sequence of transformation is observed in sulfide aggregates at the contacts of dikes at the Degdekan deposit.

According to experimental data, the solid-phase reactions involving pyrite and arsenopyrite attain equilibrium at 700°C within a few days (Barton and Skinner, 1979). No equilibrium between sulfides was achieved in most of the studied arsenopyrite-bearing assemblages at the Degdekan deposit, though the ore was heated approximately to the indicated temperature. This is supported by a wide variation in As contents in arsenopyrite and the coexistence of loellingite and pyrite. Thus, the transformation from pyrite–arsenopyrite into pyrrhotite–arsenopyrite assemblage began at ~491°C and was not completed, though the ore was heated to a temperature above 702°C, as follows from the formation of loellingite. Owing to the high rate of recrystallization, the Degdekan veins affected by thermal metamorphism have a fine-grained texture and contain nonequilibrium assemblages of arsenopyrite, pyrite, pyrrhotite, and loellingite. This testifies to a short period of heating.

The significant variations in Fe content in newly formed or recrystallized sphalerite from veins at the contact of dikes at the Degdekan deposit may be caused either by association of primary sphalerite with other Fe-bearing sulfides prior to ore heating or by possible removal of sulfur from the reaction zone due to various degrees of system isolation during heating, that is, how

well the sulfide microintergrowths were encapsulated in quartz. During the heating, sphalerite does not show a significant increase in FeS (Barton and Toulmin, 1966). However, according to experimental data (Barton and Toulmin, 1966; Scott, 1984), sphalerite associated with arsenopyrite, loellingite, and pyrrhotite in newly formed assemblages must have a higher Fe content than sphalerite from the unheated ore at the Degdekan deposit. Therefore, if sphalerite–pyrite aggregates were transformed into sphalerite–pyrrhotite assemblage as a result of thermal metamorphism, the Fe content in sphalerite should increase.

The appearance of tennantite at the boundary of arsenopyrite–sphalerite intergrowths could have been caused by interaction between arsenopyrite and emulsion chalcopyrite hosted in sphalerite. This reaction proceeds at ~400°C (Sugaki, 1957; Sakharova and Kalitkina, 1970) and may be simplified as follows:

$$FeAsS + 3CuFeS_2 \longrightarrow Cu_3AsS_3 + 4FeS.$$

Note that chalcopyrite emulsion is characteristic of sphalerite from unmetamorphosed ores and disappears in metamorphosed sphalerite.

The increase in fineness of native gold at the contact of dikes at the Degdekan deposit by 100–250 units serves as additional evidence for thermal metamorphism of the ore, although the intensity of this process could not be estimated. Experimental and empirical data (Moiseenko, 1965; Gamyanin et al., 1980; Shilo et al., 1992) have shown that native gold is transformed even at a relatively low temperature, beginning from 100°C.

The quartz veins at the Gol'tsovsky and Degdekan gold deposits were formed from aqueous–carbon dioxide solutions, as is evident from inclusions entrapped during quartz crystallization. The simultaneous capture of aqueous and carbon dioxide fluid inclusions localized in a single quartz grain testifies to the circulation of two fluids in the mineral-forming system (Ramboz et al., 1982). The formation of two immiscible fluids enriched in water and gas, respectively, may be caused by pressure release (Roedder, 1984). Pressure fluctuations owing to tectonic movements also may initiate precipitation of ore components, including gold in quartz veins (Dugdale and Hagemann, 2001).

The wide variations in fluid salinity can be explained by mixing of carbon dioxide and aqueous fluids. CO_2 supply into a fluid causes its salting out; i.e., the salinity of aqueous fluids becomes higher in comparison with carbon dioxide fluids. The lowest salinities estimated in the fluid inclusions are comparable with those at the Natalka (Eremin et al., 1994) and Nezhdaninsky (Bortnikov et al., 1998) gold–quartz deposits, the largest of the Yana–Kolyma Fold System. These estimates also fit the values accepted for metamorphic gold–quartz mineralization around the world (Phillips and Powell, 1993; Goldfarb et al., 1997).

The absence of contrasting differences in *PTX* parameters between unmetamorphosed and metamorphosed quartz veins at the studied deposits is surprising. The close melting and eutectic temperatures indicate that fluids of similar composition and salinity were captured in the inclusions of both types of veins (Table 2). The salinity of fluids virtually does not depend on the degree of metamorphism. In both cases, the composition of fluids was characterized by the prevalence of Na, K, and possibly Mg chlorides. The homogenization temperature of fluid inclusions in the metamorphosed quartz veins is only slightly higher than in the unmetamorphosed veins. The total fluid pressure in the metamorphosed veins (0.8–1.5 kbar) shows an insignificant increase in comparison with that in the unmetamorphosed veins (0.7–1.3 kbar).

An accurate pressure correction to the temperature of quartz formation may be introduced only in cases where (1) inclusions contain a pure NaCl solution, (2) the concentration of this solution has been accurately determined, and (3) the pressure of mineral formation has been reliably established (Roedder, 1984). The pressure correction to a homogenization temperature of 300°C is ~20°C for inclusions that meet the above requirements. Therefore, even if such a correction is introduced, the real temperature will be no higher than 300°C. Hence, within a pressure range of 1–1.5 kbar, the primary quartz was formed at a temperature of 170–270°C, and metamorphism shifted this temperature only by 30°C (200–300°C) with a pressure correction for 5–10 wt % NaCl equiv (Zhang and Frantz, 1987).

At the same time, the emplacement of dikes exerted an obvious thermal effect on the veins, expressed in the decrepitation of fluid inclusions and the appearance of substantially gas inclusions in the metamorphosed veins. This fact is noteworthy for estimation of postmineral metamorphism of quartz veins bearing such gas inclusions. In particular, an extremely high content of gas inclusions was established at the Ashanti deposit, Ghana (Oberthür et al., 1994). Chromatographic analysis also showed (Table 3) that the total gas content in the metamorphosed veins is 1.5–2 times lower than that in the unmetamorphosed veins. The gas component of fluids reacted first to the emplacement of dikes. The enrichment of the metamorphic fluid in CO_2 most likely is a result of intergranular migration recrystallization of gangue quartz. In particular, Klemd (1998) suggested that water, owing to its high polarity (Crawford and Hollister, 1986), remains beyond the advancing recrystallization front, thus promoting entrapment of CO_2-rich fluids. At the same time, the persistent association of recrystallized quartz with carbonate aggregates indicates that postmagmatic carbonate solutions acted as recrystallization agents.

ACKNOWLEDGMENTS

We are grateful to R.J. Newberry and A.A. Tomilenko for their participation in discussion of various aspects of this study. We also thank N.S. Bortnikov for constructive criticism that allowed us to improve the manuscript. This study was supported by the Far East Division of the Russian Academy of Sciences, project no. 06-III-A-08-352.

REFERENCES

1. B. S. Andreev, T. I. Makhorkina, S. I. Portnyagin, and E. E. Tyukova, "Thermal Metamorphism of Gold Deposits in the Northeast USSR," in *Geology and Mineral Resources of Northeastern Asia* (Far East Division, Acad. Sci. USSR, Vladivostok, 1984), pp. 164–175 [in Russian].
2. N. P. Anikeev, G. N. Gamyanin, M. L. Gelman, et al., "Relationship of Gold Mineralization with Magmatism in the Northeast of the USSR," in *Magmatism of Northeastern Asia* (Magadan, 1976), Part 3, pp. 198–206 [in Russian].
3. O. V. Babaitsev, "Xenoliths of Metamorphic Rocks in Diorite Dikes in the Southwestern Yana–Kolyma Area," in *Metallogeny of the Northeastern USSR* (Magadan, 1984), pp. 97–102 [in Russian].
4. P. B. Barton and B. J. Skinner, "Sulfide Mineral Stability," in *Geochemistry of Hydrothermal Ore Deposits* (Wiley, New York, 1979; Mir, Moscow, 1982), pp. 278–403.
5. P. B. Barton and P. Toulmin, "Phase Relations Involving Sphalerite in Fe–Zn–S System," in *Thermodynamics of Postmagmatic Processes* (Econ. Geol. **61**, 815–849, 1966; Mir, Moscow, 1968), pp. 815–849.
6. Yu. A. Bilibin, "Age of Some Gold Deposits in the Kolyma Region," Sov. Geol., No. 5/6, 182–184 (1940).
7. A. S. Borisenko, "Analysis of the Salt Composition of Fluid Inclusions Using Cryometry Technique," Geol. Geofiz. **18** (8), 16–27 (1977).
8. N. S. Bortnikov, G. N. Gamyanin, V. A. Alpatov, et al., "Mineralogy, Geochemistry and Origin of the Nezhdaninsky Gold Deposit (Sakha-Yakutia, Russia)," Geol. Rudn. Mestorozhd. **40** (2), 137–156 (1998) [Geol. Ore Deposits **40** (2), 121–138 (1998)].
9. P. E. Brown, "FLINCOR: A Microcomputer Program for the Reduction and Investigation of Fluid Inclusion Data," Am. Mineral. **74**, 1390–1393 (1989).
10. P. E. Brown and S. G. Hagemann, "MacFlinCor: A Computer Program for Fluid Inclusion Data Reduction and Manipulation," in *Fluid Inclusions in Minerals: Method and Application* (VPI Press, 1994), pp. 231–250.
11. L. A. Clark, "The Fe–As–S System: Phase Relations and Applications," in *Problems of Endogenic Deposits* (Econ. Geol. **55**, 1345–1381, 1960; Mir, Moscow, 1966), No. 3, pp. 160–250.
12. M. L. Crawford and L. S. Hollister, "Metamorphic Fluids: the Evidence from Fluid Inclusions," in *Fluid Interactions during Metamorphism* (Springer, Berlin, 1986), pp. 1–35.
13. A. L. Dugdale and S. G. Hagemann, "The Bronzewing Lode Gold Deposit, Western Australia: P–T–X Evidence for Fluid Immiscibility Caused by Cyclic Decompression in Gold-Bearing Quartz Veins," Chem. Geol. **173**, 59–90 (2001).
14. R. A. Eremin, S. V. Voroshin, V. A. Sidorov, et al., "Geology and Genesis of the Natalkinskoye Gold Deposit, Northeast Russia," Int. Geol. Review. **36**, 1113–1138 (1994).
15. L. V. Firsov, "Quartz and Gold Recrystalization in Veins of the Rodionov Deposit," in *Geology* (Tr. VNII-1, Magadan, 1956), No. 11, pp. 56–64 [in Russian].
16. L. V. Firsov, "Structure, Morphology, Mineralogy, and Mineralization of the Igumenov Gold Deposit," in *Geology* (Tr. VNII-1, Magadan, 1958), No. 33, pp. 191–262 [in Russian].
17. G. N. Gamyanin, Yu. Ya. Zhdanov, V. M. Supletsov, and G. S. Anisimov, "Specific Features of Native Gold in Primary Gold Deposits of the Verkhoyansk–Kolyma Fold System," in *Problems of Geology, Mineralogy, and Geochemistry of Gold Mineralization in Yakutia* (Yakutsk, 1980), pp. 69–80 [in Russian].
18. R. J. Goldfarb, D. L. Leach, M. L. Miller, and W. J. Pickthorn, "Geology, Metamorphic Setting, and Genetic Constraints of Epigenetic Lode-Gold Mineralization within the Cretaceous Valdez Group, South-Central Alaska," in *Turbidite-Hosted Gold Deposits* (Geol. Assoc. Canada Special Paper, 1986), Vol. 32, pp. 87–105.
19. R. J. Goldfarb, L. D. Miller, D. L. Leach, and L. W. Snee, "Gold Deposits in Metamorphic Rocks of Alaska," Econ. Geol. Monog. **9**, 151–190 (1997).
20. M. l. Greninger, S. L. Klemperer, and W. J. Nokleberg, *Geographic Information System (GIS) Compilation of Geophysical, Geologic, and Tectonic Data for the Circum-North Pacific* (USGS Open-File Report 99-422, Version 1.0, 1999).
21. A. J. Hall, "Pyrite–Pyrrhotine Redox Reactions in Nature," Mineral. Mag. **50**, 223–229 (1986).
22. V. A. Kalyuzhny, *Principles of the Theory of Mineral-Forming Fluids* (Naukova Dumka, Kiev, 1982) [in Russian].
23. A. N. Kirgintsev, L. N. Trushnikova, and V. G. Lavrent'eva, *Solubility of Inorganic Substances in Water* (Khimiya, Leningrad, 1972) [in Russian].
24. R. Klemd, "Comment on the Paper by Schmidt, Mumm, et al.: High CO_2 Content of Fluid Inclusions in Gold Mineralisations in the Ashanti Belt, Ghana: A New Category of Ore-Forming Fluids," Miner. Deposita **33**, 317–319 (1998).
25. Vl. K. Kozlov, E. E. Tyukova, V. Ya. Borkhodoev, and Vik. K. Kozlov, *Arsenopyrite Subsolidus Phase Relationships at a Temperature below 400°C in Pseudobinary Pyrite-Loellingite System*, Available from VAll-Russia Institute of Scientific and Technical Information, No. 5171-B86 (Moscow, 1986) [in Russian].
26. G. Kullerud and H. S. Yoder, "Pyrite Stability Relations in the Fe–S System," in *Problems of Endogenic Deposits* (Econ. Geol. **54**, 533–572, 1959; Mir, Moscow, 1966), No. 3, pp. 71–131.
27. V. G. Moiseenko, *Metamorphism of Gold Deposits in the Amur Region* (Khabarovsk, 1965) [in Russian].
28. T. Oberthür, U. Vetter, A. S. Mumm, et al., "The Ashanti Gold Mine at Obuasi, Ghana: Mineralogical, Geochemical, Stable Isotope and Fluid Inclusion Studies on the

Metallogenesis of the Deposit," Geol. Jb. Hannover. Ser. D **100**, 31–129 (1994).

29. N. Yu. Osorgin, *Chromotographic Analysis of Gas Phase in Minerals* (UIGGM, Novosibirsk, 1990) [in Russian].
30. N. Yu. Osorgin and A. A. Tomilenko, USSR Inventor's Certificate No. 1562816, 1990a.
31. N. Yu. Osorgin and A. A. Tomilenko, USSR Inventor's Certificate No. 1592678, 1990b.
32. G. N. Phillips and R. Powell, "Link between Gold Provinces," Econ. Geol. **88**, 1084–1098 (1993).
33. C. Ramboz, M. Pichavant, and A. Weisbrod, "Fluid Immiscibility in Natural Processes: Use and Misuse of Fluid Inclusion Data. II: Interpretation of Fluid Inclusion Data in Terms of Immiscibility," Chem. Geol. **37**, 29–48 (1982).
34. E. Roedder, *Fluid Inclusions in Minerals* (Reviews in Mineralogy, Mineral. Soc. Amer., 1984, Vol. 12; Mir, Moscow, 1987).
35. E. Roedder and R. J. Bodnar, "Geologic Pressure Determinations from Fluid Inclusion Studies," Ann. Rev. Earth Planet. Sci. **8**, 263–301 (1980).
36. M. S. Sakharova and N. A. Kalitkina, "Study of the Tennantite and Enargite Formation by Heating of Chalcopyrite and Arsenopyrite Ores," Vestn. Mosk. Univ., Ser. 4, Geol., No. 6, 50–58 (1970).
37. V. D. Scott, "Usage of Sphalerite and Arsenopyrite for Evaluation of Temperature and Sulfur Activity in Hydrothermal Deposits," in *Physicochemical Models of Petrogenesis and Ore Formation* (Nauka, Novosibirsk, 1984), pp. 41–49 [in Russian].
38. N. A. Shilo, *Geologic Structure and Sources of the Yana–Kolyma Placer Gold Belt* (Tr. VNII-1, Magadan, 1960), No. 63 [in Russian].
39. N. A. Shilo, V. I. Goncharov, A. V. Alshevsky, and V. V. Vortsepnev, *Formation Conditions of Gold Mineralization in the Structural Units of the Northeastern USSR* (Nauka, Moscow, 1988) [in Russian].
40. N. A. Shilo, M. S. Sakharova, N. N. Krivitskaya, et al., *Mineralogy and Genesis of Gold–Silver Mineralization in the Northwestern Pacific Framework* (Nauka, Moscow, 1992) [in Russian].
41. P. I. Skornyakov, "Age of Gold Mineralization in Northeastern USSR," in *Proceedings on Geology of the Northeastern USSR* (Sov. Kolyma, Magadan, 1949), No. 5, pp. 13–21 [in Russian].
42. A. Sugaki, "Thermal Studies on the Diffusion between Some Sulphide Minerals in the Solid Phase," Sci. Repts. Tohoku Univ. Ser. 3 **5**, 95–112 (1957).
43. *Tectonics, Geodynamics, and Metallogeny of the Republic of Sakha (Yakutia)*, Ed. by L. M. Parfenov and M. I. Kuz'min (Nauka/Interperiodika, Moscow, 2001) [in Russian].
44. N. B. Vargaftik, *Tables of the Thermophysical Properties of Liquids and Gases*, 2nd ed. (Nauka, Moscow, 1972; Halsted Press, New York, 1975).
45. S. V. Voroshin, "Relationship between Ore Mineralization and Dikes at the Degdekan Deposit," Geol. Rudn. Mestorozhd., **30** (4), 30–37 (1988).
46. S. V. Voroshin and N. I. Eremin, "Sulfide Mineral Associations at the Gold Deposits of the Upper Kolyma Region," Vestn. Mosk. Univ., Ser. 4, Geol., No. 2, 60–74 (1995).
47. S. D. Voznesensky, V. A. Ogorodov, N. G. Mannafov, et al., *Explanatory Notes to the Geological Map and Map of Mineral Resources of the Okhotsk–Kolyma Region on a Scale 1 : 500000, in 4 Books* (Magadan, 1999) [in Russian].
48. Y.-G. Zhang and J. D. Frantz, "Determination of the Homogenization Temperatures and Densities of Supercritical Fluids in the System NaCl–KCl–$CaCl_2$–H_2O Using Synthetic Fluid Inclusions," Chem. Geol. **64**, 335–350 (1987).